

CD8 T cells compensate for impaired humoral immunity in COVID-19 patients with hematologic cancer

Erin Bange

University of Pennsylvania

Nicholas Han

University of Pennsylvania <https://orcid.org/0000-0003-1410-9931>

E. Paul Wileyto

University of Pennsylvania

Justin Kim

University of Pennsylvania <https://orcid.org/0000-0003-0774-8137>

Sigrid Gouma

University of Pennsylvania <https://orcid.org/0000-0002-7853-8340>

James Robinson

University of Pennsylvania

Allison Greenplate

University of Pennsylvania

Florence Porterfield

University of Pennsylvania

Olutosin Owoyemi

University of Pennsylvania

Karan Naik

University of Pennsylvania

Cathy Zheng

University of Pennsylvania <https://orcid.org/0000-0002-0092-5463>

Michael Galantino

University of Pennsylvania

Ariel Weisman

University of Pennsylvania <https://orcid.org/0000-0002-7187-304X>

Carolin Ittner

University of Pennsylvania

Emily Kugler

University of Pennsylvania

Amy Baxter

UPenn <https://orcid.org/0000-0002-1555-0713>

Madison Weirick

University of Pennsylvania

Christopher McAllister

University of Pennsylvania

Ngolela Esther Babady

Memorial Sloan Kettering Cancer Center

Anita Kumar

Memorial Sloan Kettering

Adam Widman

Memorial Sloan Kettering Cancer Center

Susan Dewolf

Memorial Sloan Kettering

Sawsan Boutemine

Memorial Sloan Kettering

Charlotte Roberts

University of Pennsylvania

Krista Budzik

University of Pennsylvania

Susan Tollett

University of Pennsylvania

Carla Wright

University of Pennsylvania

Tara Perloff

University of Pennsylvania

Lova Sun

University of Pennsylvania

Divij Mathew

University of Pennsylvania <https://orcid.org/0000-0002-8323-7358>

Josephine Giles

University of Pennsylvania

Derek Oldridge

University of Pennsylvania <https://orcid.org/0000-0003-2177-5633>

Jennifer Wu

University of Pennsylvania

Cecile Alanio

University of Pennsylvania <https://orcid.org/0000-0003-2785-7445>

Sharon Adamski

University of Pennsylvania

Laura Vella

Children's Hospital of Philadelphia

Samuel Kerr

University of Pennsylvania

Justine Cohen

Massachusetts General Hospital

Randall Oyer

University of Pennsylvania <https://orcid.org/0000-0001-7554-4166>

Ryan Massa

University of Pennsylvania

Ivan Maillard

University of Pennsylvania

Kara Maxwell

University of Pennsylvania <https://orcid.org/0000-0001-8192-4202>

Peter Maslak

MSKCC

Robert Vonderheide

University of Pennsylvania

Jedd D. Wolchok

Memorial Sloan Kettering Cancer Center <https://orcid.org/0000-0001-6718-2222>

Scott Hensley

University of Pennsylvania <https://orcid.org/0000-0002-2928-7506>

E. Wherry

University of Pennsylvania <https://orcid.org/0000-0003-0477-1956>

Nuala Meyer

UPenn

Angela DeMichele

University of Pennsylvania Perelman School of Medicine <https://orcid.org/0000-0003-1297-4251>

Oluwatosin Oniyide

University of Pennsylvania

Roseline Agyekum

University of Pennsylvania

Thomas Dunn

University of Pennsylvania

Tiffanie Jones

University of Pennsylvania Perelman School of Medicine

Heather Giannini

University of Pennsylvania

Alfred Garfall

University of Pennsylvania

John Reilly

UPenn

Santosha Vardhana

Memorial Sloan Kettering

Ronac Mamtani

University of Pennsylvania

Alexander Huang (✉ alexander.huang@penmedicine.upenn.edu)

University of Pennsylvania <https://orcid.org/0000-0002-0099-0492>

Article

Keywords: COVID-19, hematologic cancer, CD8 T cells

Posted Date: February 2nd, 2021

DOI: <https://doi.org/10.21203/rs.3.rs-162289/v1>

License:   This work is licensed under a Creative Commons Attribution 4.0 International License.

[Read Full License](#)

Version of Record: A version of this preprint was published at Nature Medicine on May 20th, 2021. See the published version at <https://doi.org/10.1038/s41591-021-01386-7>.

1 **CD8 T cells compensate for impaired humoral immunity in COVID-19 patients with**
2 **hematologic cancer**

3
4 Erin M. Bange*^{1,2}, Nicholas A. Han*^{1,3}, Paul Wileyto^{2,7}, Justin Y. Kim^{1,3}, Sigrid Gouma¹⁶, James
5 Robinson², Allison R. Greenplate^{3,13}, Florence Porterfield¹, Olutosin Owoyemi¹, Karan Naik¹, Cathy
6 Zheng², Michael Galantino², Ariel R. Weisman⁹, Caroline A.G. Ittner⁹, Emily M. Kugler¹, Amy E.
7 Baxter^{3,13}, Olutwatosin Oniyide⁹, Roseline S. Agyekum⁹, Thomas G. Dunn⁹, Tiffanie K. Jones⁹, Heather
8 M. Giannini⁹, Madison E. Weirick¹⁶, Christopher M. McAllister¹⁶, N. Esther Babady^{5,6}, Anita Kumar⁵, Adam
9 J Widman⁵, Susan DeWolf⁹, Sawsan R Boutemine⁵, Charlotte Roberts², Krista R Budzik², Susan Tollett²,
10 Carla Wright², Tara Perloff^{2,11}, Lova Sun^{1,2}, Divij Mathew^{3,13}, Josephine R. Giles^{3,13,15}, Derek A.
11 Oldridge^{3,14}, Jennifer E. Wu^{3,13,15}, Cécile Alanio^{3,13,15}, Sharon Adamski^{3,13}, Alfred L. Garfall^{1,2}, Laura
12 Vella¹⁷, Samuel J. Kerr^{2,12}, Justine V. Cohen^{2,11}, Randall A. Oyer^{2,12}, Ryan Massa^{1,2,10}, Ivan P. Maillard^{1,2},
13 The UPenn COVID Processing Unit, Kara N. Maxwell^{1,2}, John P. Reilly⁹, Peter G. Maslak^{5,6}, Robert H.
14 Vonderheide^{2,3,15}, Jedd D. Wolchok^{4,5}, Scott E. Hensley^{3,16}, E. John Wherry^{3,13,15}, Nuala Meyer^{3,9}, Angela
15 M. DeMichele^{1,2}, Santosha A. Vardhana^{±*4,5,15}, Ronac Mamtani^{±*1,2}, Alexander C. Huang^{±*1,2,3,15}

16 ¹ Division of Hematology/Oncology, Department of Medicine, Perelman School of Medicine, University of
17 Pennsylvania

18 ² Abramson Cancer Center, University of Pennsylvania

19 ³ Institute for Immunology, Perelman School of Medicine, University of Pennsylvania

20 ⁴ Human Oncology and Pathogenesis Program, Memorial Sloan Kettering Cancer Center

21 ⁵ Department of Medicine, Memorial Sloan Kettering Cancer Center

22 ⁶ Department of Laboratory Medicine, Memorial Sloan Kettering Cancer Center

23 ⁷ Department of Biostatistics, Epidemiology, and Informatics, Perelman School of Medicine, University of
24 Pennsylvania

25 ⁸ Division of Hematology/Oncology, Department of Medicine, Perelman School of Medicine, Presbyterian
26 Hospital

27 ⁹ Division of Pulmonary and Critical Care, Department of Medicine, Perelman School of Medicine,
28 University of Pennsylvania

29 ¹⁰ Division of Hematology/Oncology, Department of Medicine, Perelman School of Medicine, Presbyterian
30 Hospital

31 ¹¹ Division of Hematology/Oncology, Department of Medicine, Perelman School of Medicine,
32 Pennsylvania Hospital

33 ¹² Division of Hematology/Oncology, Department of Medicine, Lancaster General Hospital

34 ¹³ Department of Systems Pharmacology and Translational Therapeutics, Perelman School of Medicine,
35 University of Pennsylvania

36 ¹⁴ Department of Pathology and Laboratory Medicine, Perelman School of Medicine, University of
37 Pennsylvania

38 ¹⁵ Parker Institute for Cancer Immunotherapy

39 ¹⁶ Department of Microbiology, Perelman School of Medicine, University of Pennsylvania

40 ¹⁷ Department of Pediatrics, Perelman School of Medicine, Children's Hospital of Philadelphia

41
42 * These authors contributed equally to this work

43
44 ± Co-Corresponding author(s): Address correspondence to S.V. (vardhans@mskcc.org), R.M.
45 (ronac.mamtani@penmedicine.upenn.edu), or A.C.H. (alexander.huang@penmedicine.upenn.edu)

46

47 **Abstract**

48 Cancer patients have increased morbidity and mortality from Coronavirus Disease 2019
49 (COVID-19), but the underlying immune mechanisms are unknown. In a cohort of 100 cancer
50 patients hospitalized for COVID-19 at the University of Pennsylvania Health System, we found
51 that patients with hematologic cancers had a significantly higher mortality relative to patients
52 with solid cancers after accounting for confounders including ECOG performance status and
53 active cancer status. We performed flow cytometric and serologic analyses of 106 cancer
54 patients and 113 non-cancer controls from two additional cohorts at Penn and Memorial Sloan
55 Kettering Cancer Center. Patients with solid cancers exhibited an immune phenotype similar to
56 non-cancer patients during acute COVID-19 whereas patients with hematologic cancers had
57 significant impairment of B cells and SARS-CoV-2-specific antibody responses. High
58 dimensional analysis of flow cytometric data revealed 5 distinct immune phenotypes. An
59 immune phenotype characterized by CD8 T cell depletion was associated with a high viral load
60 and the highest mortality of 71%, among all cancer patients. In contrast, despite impaired B cell
61 responses, patients with hematologic cancers and preserved CD8 T cells had a lower viral load
62 and mortality. These data highlight the importance of CD8 T cells in acute COVID-19,
63 particularly in the setting of impaired humoral immunity. Further, depletion of B cells with anti-
64 CD20 therapy resulted in almost complete abrogation of SARS-CoV-2-specific IgG and IgM
65 antibodies, but was not associated with increased mortality compared to other hematologic
66 cancers, when adequate CD8 T cells were present. Finally, higher CD8 T cell counts were
67 associated with improved overall survival in patients with hematologic cancers. Thus, CD8 T
68 cells likely compensate for deficient humoral immunity and influence clinical recovery of COVID-
69 19. These observations have important implications for cancer and COVID-19-directed
70 treatments, immunosuppressive therapies, and for understanding the role of B and T cells in
71 acute COVID-19.

72 **Main Text**

73 Severe illness affects up to 20% of those hospitalized with Coronavirus Disease 2019 (COVID-
74 19)¹ and is manifested by acute respiratory distress syndrome (ARDS), multi-organ failure,
75 and/or death². Severe disease has been linked to immune dysregulation, including deficiency in
76 the production of type I and type III interferons³⁻⁵, marked lymphopenia⁶⁻¹⁰, and a paradoxical
77 increase in pro-inflammatory cytokines, such as TNF α , IL-1 β , and IL-6^{3, 6, 11-15}. In addition,
78 alteration of the lymphocyte compartments has been reported during COVID-19 with increases
79 in activated CD4 and CD8 T cells¹⁵⁻¹⁸, skewing of CD8 T cells towards effector^{16, 17} and
80 exhausted phenotypes¹⁸, and increased differentiation of CD4 T cells towards the Th17
81 lineage^{17, 19}. Despite these marked alterations in their T cell compartment, COVID-19 patients
82 have robust plasmablast responses^{15, 20}, and the majority of patients generate IgM and IgG
83 antibodies to SARS-CoV-2 over the course of disease²⁰⁻²². More recently, integrated and multi-
84 omic analyses have highlighted the tremendous heterogeneity of the human immune response
85 to SARS-CoV-2, with distinct immunophenotypes that are associated with COVID-19 disease
86 severity and disease trajectory^{5, 11, 12, 15, 16}. Understanding how clinical features, particularly
87 patient comorbidity, impact host immune responses to SARS-CoV-2 will elucidate determinants
88 of immunotype and disease severity.

89 Cancer patients have an increased risk of severe illness from COVID-19²³⁻²⁶ with an
90 estimated case fatality rate of 25%²⁷ compared to 2.7% in the general population²⁸. Importantly,
91 cancer is a heterogeneous disease with even higher mortality rates reported for patients with
92 particular subtypes of cancer. For example, several cohort and registry studies have
93 demonstrated particularly poor outcomes among patients with hematologic cancers, with
94 mortality rates as high as 55%^{23, 26, 29-37}. However, it remains unknown whether the increased
95 mortality by cancer subtype is independent of the confounding effects of other prognostic factors
96 such as Eastern Cooperative Oncology Group (ECOG) performance status, active cancer

97 status, and cancer therapy. Further, data is limited on the immune landscape of cancer patients;
98 whether components of cellular and humoral immunity are compromised, the impact of immune-
99 modulating therapies such as B cell depleting therapy, and how these factors influence mortality
100 in the setting of COVID-19 is also not known. To address these questions, we studied three
101 cohorts of cancer patients with acute COVID-19 across two hospital systems to understand the
102 immunologic determinants of COVID-19 mortality in cancer.

103 **Hematologic cancer is an independent risk factor of COVID-19 mortality**

104 To understand the clinical impact of COVID-19 on cancer patients, we first conducted a
105 prospective multi-center observational cohort study of cancer patients hospitalized with COVID-
106 19 (COVID-19 Outcomes in Patients with Cancer, COPE). Between April 28 and September 15
107 2020, 114 patients with history of hematologic or solid tumor malignancy, and laboratory-
108 confirmed SARS-CoV-2 infection or presumed COVID-19 diagnosis, were enrolled across 4
109 hospitals in the University of Pennsylvania Health System. 14 patients were excluded from the
110 analyses due to either low suspicion for COVID-19 infection, or benign tumor diagnosis. The
111 median age of this cohort was 68 years, 52% were male, 54% Black, and 57% were current or
112 former smokers (**Table 1**), reflecting the demographics of severe COVID-19^{38, 39}. In terms of
113 cancer-specific factors, 78% of patients had solid cancers, with prostate and breast cancers
114 most prevalent; 46% had active cancer, defined as diagnosis or treatment within 6 months; and
115 49% had a recorded ECOG performance status of 2 or higher (**Table 1**). During follow up, 48%
116 of subjects required ICU level care, and 38% of patients died within 30 days of admission
117 (**Table 2**), consistent with previously reported rates for severe COVID-19 in this population^{30, 34,}
118 ³⁷.

119 To understand key determinants of COVID-19 disease severity, we performed univariate
120 analysis to identify factors associated with all-cause mortality within 30 days of discharge. We
121 included relevant covariates, including patient factors such as age, race, gender, and smoking

122 history (ever versus never)^{2, 38–40}; cancer-specific factors including ECOG performance status³⁵,
123 status of cancer (e.g., active versus remission)^{36, 36}; cancer type (e.g., heme versus solid
124 cancer)^{29, 34, 36, 41, 42}; and cancer treatment^{26, 37}. Increased mortality was significantly associated
125 with prior or current smoking ($p = 0.028$), poor ECOG performance (ECOG 3-4, $p=0.001$), and
126 active cancer status ($p=0.024$) (**Fig. 1**). In addition, patients with hematologic cancers (mostly
127 lymphoma and leukemia), appeared to have an increased risk of mortality relative to solid
128 cancers (54% versus 33% respectively, $p=0.075$) (**Table 3**). This is consistent with recent data
129 showing increased disease severity and mortality in patients with hematologic malignancies^{23, 29,}
130 ^{34–36, 41}. Notably, cancer treatment, including cytotoxic chemotherapy, was not significantly
131 associated with COVID-19 mortality, also consistent with published literature in patients with
132 cancer^{29, 30, 34, 36, 41}.

133 To determine whether the increased mortality observed in patients with hematologic
134 malignancy was independent of potential confounding effects from smoking history, poor ECOG
135 performance, and active cancer, which were not corrected for in the prior studies, we performed
136 multivariable logistic regression. Patients with hematologic cancers tended to be younger, male,
137 less likely to have coexisting comorbidities, and more likely to have received recent cytotoxic
138 chemotherapy (**Supplemental Table 1**). In this fully adjusted analysis, hematologic malignancy
139 was strongly associated with mortality, in comparison to solid cancer (OR 3.3, 95% CI 1.01-
140 10.8, $p=0.048$) (**Table 3**). Similar results were observed in time-to-event analyses using Kaplan
141 Meyer methods (**Fig. 2a**, median overall survival (mOS) not reached for patients with solid
142 cancers vs 47 days for patients with heme cancers, p -value=0.030) and Cox regression models
143 (**Table 3**, HR 2.56, 95% CI 1.19-5.54, $p=0.017$). Moreover, patients with hematologic cancers
144 had higher levels of many inflammatory markers on admission laboratory testing, including
145 ferritin, IL-6, and LDH (**Fig. 2b**). There were no significant differences in CRP, fibrinogen, D-
146 dimer, lymphocyte counts, and neutrophil counts, while ESR was higher in patients with solid

147 cancer (**Extended Data Fig. 1 a,b**). Thus, hematologic malignancy was an independent risk
148 factor of death, with signs of a dysregulated inflammatory response.

149 **Hematologic cancer patients have an impaired SARS-CoV2-specific antibody response.**

150 To understand the immune landscape in cancer patients, as compared to patients without
151 cancer, we leveraged an observational study of hospitalized COVID-19 patients at the
152 University of Pennsylvania Health System where blood was collected (MESSI-COVID)¹⁵. This
153 analysis included 130 subjects with flow cytometric and/or serologic analysis. In particular, we
154 focused on 22 subjects with active cancer (**Supplemental Tables 2, 3**), including patients
155 undergoing cancer-directed therapies such as chemotherapy, immunotherapy, or B cell directed
156 therapies (**Supplemental Table 4**). Age, gender, and race were similarly distributed in COVID-
157 19 patients with active cancer and those without, and both groups had a similar timeframe of
158 symptom onset and disease severity (**Fig. 3a, Supplemental Table 2**). However, cancer
159 patients had a higher all-cause mortality (36.4% versus 11.1%, **Fig. 3a**), consistent with our
160 COPE clinical cohort, and what has been reported in other cohorts of COVID-19 patients^{23, 26, 29,}
161 ³⁰.

162 As humoral immunity is critical for protective immunity against SARS-CoV-2, we
163 hypothesized that a defect in SARS-CoV-2-specific antibodies may be associated with the
164 increase in mortality seen in patients with active cancer. We assessed the levels of IgM and IgG
165 antibodies that recognized the SARS-CoV-2 receptor binding domain (RBD), using an enzyme-
166 linked immunosorbent assay (ELISA) based approach^{43, 44}. Cancer patients had significantly
167 decreased SARS-CoV-2-specific IgG and IgM responses compared to non-cancer patients
168 (**Extended Data Fig. 2a**). These differences were not due to the timing of SARS-CoV-2
169 infection as time from symptom onset was similar (**Supplemental Table 2**). As hematologic
170 malignancies directly involve the lymphoid and myeloid immune compartments, we suspected
171 that hematologic cancers may have an impaired humoral immunity against SARS-CoV-2.

172 Indeed, the vast majority of hematologic cancer patients (6/7) had IgM and IgG levels below the
173 cutoff of positivity of 0.48 arbitrary units (**Fig. 3b, Extended Data Fig. 2b**). In contrast, those
174 with solid cancers had IgG and IgM antibody responses that were more comparable to patients
175 without cancer (**Fig. 3b**).

176 **A T cell-depleted immune phenotype is associated with COVID-19 mortality.**

177 Protective antibody responses require effective T cell and B cell responses. We therefore
178 examined whether cancer patients had an altered cellular response to SARS-CoV-2. We first
179 performed exploratory high-dimensional analysis on the lymphocyte compartment of 45 patients
180 with COVID-19 including 37 non-cancer, 6 solid cancer, and 2 hematologic cancer patients.
181 UMAP (Uniform Manifold Approximation and Projection) representation of 27-parameter flow
182 cytometry data highlighted discrete islands of CD4 and CD8 T cells, and CD19+ B cells
183 (**Extended Data Fig. 3a and Fig. 3c**). To understand whether there were major global
184 differences in lymphocytes between solid, hematologic, and non-cancer patients, we used the
185 Earth Mover's Distance (EMD) metric⁴⁵ to calculate the distance between the UMAP projections
186 for every pair of patients. Clustering on EMD values identified 5 clusters of patients with similar
187 lymphocyte profiles (**Fig. 3c**). Differences between these clusters of patients were driven by
188 both the distribution (**Fig. 3d**) and phenotype (**Extended Data Fig. 3b and Fig. 3e**) of CD4,
189 CD8, and B cells. EMD cluster 1 was defined by depleted CD4 and B cells, increased CD8 T
190 cells, and increased activation and effector markers, including PD-1, CX3CR1, Ki67, and HLA-
191 DR (**Extended Data Fig. 3b and Fig. 3 d,e**). EMD cluster 3 had decreased T cell and B cells,
192 with an inactivated immune profile, and EMD Cluster 5 was depleted of both CD4 and CD8 T
193 cells, but had preserved B cells. In contrast, EMD cluster 4 was defined by robust
194 CCR7+CD27+ memory CD4 T cell responses and heterogenous B cell responses; EMD cluster
195 2 had the most balanced responses, with CD4, CD8, and B cells represented (**Fig. 3d,e and**
196 **Extended Data Fig. 3b**). We then correlated these 5 patterns of immune responses with clinical

197 and serological variables. EMD cluster 5 patients with depleted T cells had the highest mortality
198 and disease severity, despite generating SARS-CoV-2-specific IgM and IgG antibodies (**Fig. 3f**,
199 **Extended Data Fig. 5d**). In contrast, EMD clusters 2 and 4, with robust CD4 and/or CD8 T cell
200 responses, had the lowest mortality and a low disease severity (**Fig. 3f**, **Extended Data Fig.**
201 **5d**). These findings suggest a key role for T-cell immunity in facilitating viral clearance, even in
202 the presence of intact humoral immunity.

203 **Distinct immune landscape in hematologic cancer compared to solid cancer or no** 204 **cancer.**

205 To further understand the immune response of patients with cancer and COVID-19, we explored
206 the role of cancer subtype (solid tumor versus hematologic) on immune phenotype. Four out of
207 the 6 solid cancer patients were in EMD cluster 2, with a balanced immune phenotype (**Fig. 3e**).
208 In contrast, both hematologic cancer patients were in EMD cluster 1, which had marked
209 depletion of CD4 and B cells. Indeed, UMAP projections showed that while solid cancer patients
210 had an immune landscape similar to non-cancer patients, the two hematologic cancer patients
211 demonstrated loss of islands associated with CD4 and B cells (**Fig. 3g**). We then extended this
212 analysis by measuring the frequency and phenotype of key lymphocyte populations in the entire
213 MESSI-COVID cohort and healthy donor controls. COVID-19 patients with hematologic cancers
214 had a significantly lower frequency of CD4 and B cells compared to solid cancer patients, non-
215 cancer patients, and healthy donors without COVID-19 (**Fig. 3h**). As T follicular helper cells
216 (Tfh) and plasmablasts are critical in the generation of effective antibody responses, we
217 assessed circulating Tfh and plasmablast responses. Although limited by sample size, patients
218 with hematologic cancers had low circulating Tfh (PD1⁺ CXCR5⁺) and plasmablast responses
219 (CD19⁺CD27^{hi}CD38^{hi}), and decreased CD138 expression (**Extended Data Fig. 4a**). Thus,
220 patients with hematologic malignancy appear to have quantitative defects in CD4 and B cells
221 that may be required for effective SARS-CoV-2-specific antibody responses.

222 Patients with hematologic cancers had a preserved frequency of CD8 T cells. Therefore,
223 we wanted to determine whether there were qualitative changes within the CD8 T cell
224 compartment. We performed FlowSOM clustering analysis on non-naïve CD8 T cells from 118
225 COVID-19 patients and 30 healthy donors and visualized the clusters using UMAP. UMAP
226 clearly separated CX3CR1 and Tbet expressing effector cells from memory CD8 T cells
227 expressing CD27 and TCF-1 (**Extended Data Fig. 4b and Fig. 3i**). The effector island was
228 composed of CD45RA^{lo}CD27^{lo} effector memory cells (clusters 2 and 3) and CD45RA⁺ TEMRA
229 cells (cluster 1). The memory island was composed of CCR7^{lo} transitional memory (cluster 5),
230 and effector memory cells (clusters 7 and 8), and CCR7^{hi} central memory cells (cluster 9).
231 Activated cells, characterized by high HLA-DR, CD38, and Ki67 expression, were identified in
232 clusters 3, 4, and 5 (**Extended Data Fig. 4c**). Stem cell memory cells (cluster 10) and
233 exhausted phenotype CD8 T cells (cluster 6) were present, but at low frequencies of below
234 0.5% (**Data not shown**).

235 We then compared the landscape of CD8 T cells in patients with and without cancer.
236 CD8 T cell subsets including central memory, effector memory, transitional memory and EMRA,
237 were similar between patients with and without cancer (**Extended Data Fig. 4d**). However,
238 UMAP representation of non-naïve CD8 data demonstrated preferential enrichment of cells
239 expressing HLA-DR and CD38 in cancer patients compared to non-cancer patients (**Fig. 3j**).
240 Indeed, cancer patients had higher frequencies of activated HLA-DR, CD38, and Ki67-
241 expressing FlowSOM clusters (clusters 3, 4, and 5) compared to non-cancer patients and
242 healthy donors (**Extended Data Fig. 4e and Fig. 3k**). When stratified by cancer type, the
243 increased HLA-DR and CD38 expression was restricted to the patients with hematologic
244 cancers; patients with solid cancers and those without cancer had comparable levels of
245 activation (**Fig. 3l**). Altogether, solid cancer patients with COVID-19 had an immune landscape
246 similar to non-cancer COVID-19 patients. In contrast, patients with hematologic malignancies
247 had defects in CD4, B cells, and humoral immunity but preserved and highly activated CD8 T

248 cells, suggesting that CD8 T cells might at least partially compensate for blunted humoral
249 immune responses in patients with hematologic malignancies.

250 **CD8 T cell adequacy increases survival in the setting of impaired B cell and humoral**
251 **immunity in hematologic cancer.**

252 Patients with hematologic cancer had significantly impaired humoral immunity and a mortality
253 rate of 55% (**Table 2**). We hypothesized that CD8 T cells partially compensated for defective
254 humoral immunity and influenced survival in acute COVID-19. We tested this hypothesis in a
255 cohort of cancer patients hospitalized with COVID-19 at the Memorial Sloan Kettering Cancer
256 Center (MSKCC), which included a larger number of hematologic malignancies patients,
257 including those treated with B cell depleting therapy. This cohort included 39 solid cancer
258 patients and 45 hematologic cancer patients. The median age was 65 years, and in contrast to
259 the MESSI cohort at Penn, 81% of the cohort was white (**Fig. 4a, Supplementary Table 5,6**). A
260 significant portion of patients were treated with remdesivir and convalescent plasma – 21.4%,
261 and 46.4%, respectively (**Supplementary Table 5**). Consistent with the Penn COPE and
262 MESSI cohorts, patients with hematologic cancers did poorly, with a mortality rate of 44.4%
263 (**Fig. 4a, Supplementary Table 5**). Clinical grade 12-parameter flow cytometry and serologic
264 testing for SARS-CoV-2-specific antibodies were performed. In the MSKCC cohort, both CD4
265 and CD8 T cells were significantly decreased in patients with active solid and hematologic
266 cancers, compared with patients in clinical remission (**Extended Data Fig. 5a**). Moreover,
267 despite the fact that a substantial number of patients with hematologic cancers from the MSKCC
268 cohort received convalescent plasma, they had a significant defect in SARS-CoV-2-specific IgG
269 and IgM responses as compared to solid cancers (**Extended Data Fig. 5b**). This was
270 independent of disease severity and viral load, as assessed by RT-PCR cycle threshold.
271 (**Extended Data Fig. 5c,d**).

272 We performed high dimensional analyses on flow cytometry data that included

273 information on CD4 T cells, CD8 T cells, and B cells. EMD and clustering of 20 solid cancer, 31
274 hematologic cancer, and 6 remission patients identified 4 immune phenotypes (**Extended Data**
275 **Fig. 6a,b and Fig. 4b,c**) that corresponded to the immune phenotypes 1,2,4, and 5 identified in
276 the Penn-MESSI cohort (**Fig. 3c,d**). The Penn phenotype 3, the only cluster that did not have
277 cancer patients, was not identified in the MSKCC cancer cohort. Consistent with the Penn data,
278 MSKCC EMD cluster 5, with depleted of CD4 and CD8 T cells and preserved B cells, had the
279 highest mortality of 71%, and was associated with a high disease severity and viral load (**Fig**
280 **4d**).

281 Intriguingly, the clinical outcomes of patients with immune phenotype 4 was the greatest
282 contributor to the overall mortality difference between patients with solid and liquid cancers;
283 hematologic cancer patients with phenotype 4 had a mortality of 61% versus 9% in patients with
284 solid cancers (**Extended Data Fig. 7a**), with a corresponding higher viral load as assessed by
285 RT-PCR threshold cycle (**Extended Data Fig. 7b**). Immune phenotype 4 was characterized by
286 robust CD4 responses and decreased, but still intact, CD8 responses (**Extended Data Fig 6b**).
287 Within immune phenotype 4, patients with solid and hematologic cancers had similar CD4 and
288 CD8 T cell counts (**Extended Data Figure 7c**). However, patients with hematologic cancers had
289 near-complete abrogation of B cells (phenotype 4A), that corresponded with a mortality rate of
290 61% (**Extended Fig 7a and d**). In contrast, patients with solid cancers had intact B cells counts
291 (phenotype 4B, **Extended Data Fig 7a and d**), with a mortality of 9%. Thus, in a setting with
292 similar CD4 and CD8 T cell numbers, B cell depletion was associated with higher mortality; B
293 cells, therefore, likely play an important role in acute COVID-19.

294 Anti-CD20 therapy (α CD20) with rituximab or obinutuzumab-containing regimens
295 depleted B cells with near-complete abrogation of SARS-CoV-2-specific IgG and IgM responses
296 (**Fig. 4e**). Notably, hematologic cancer patients on chemotherapy and solid cancer patients on
297 immune checkpoint blockade also had significant depletion of B cells (**Extended Data Fig. 8a**).

298 α CD20 therapy was not associated with quantitative changes in CD4 and CD8 T cells. However,
299 patients treated with anti-CD20 therapy displayed dramatic reduction in CD4 and CD8 naïve
300 and memory T cells, instead skewing towards effector differentiation and an activated HLA-
301 DR+CD38+ phenotype (**Extended Data Fig. 8b,c**). Importantly, despite the loss of B cells and
302 humoral immunity, α CD20 therapy was not associated with increased mortality, disease
303 severity, or viral load when compared to chemotherapy or observation (**Fig. 4f**).

304 We sought to understand why α CD20 therapy was not associated with greater mortality
305 in these patients. Patients treated with α CD20 therapy were restricted to immune phenotypes 1
306 and 4, characterized by depleted B cells (**Fig 4g**). However, phenotype 1, characterized by
307 preserved CD8 T cells, was associated with a lower mortality (**Fig 4h**). Indeed, α CD20 treated
308 patients who survived their COVID-19 hospitalization had higher CD8 T cell counts (**Fig 4i**), and
309 lower viral load (**Extended Data Fig. 9a**). We extended these analyses to other patients with
310 hematologic cancers, including those on chemotherapy who also had quantitative (**Extended**
311 **Data Fig. 8a**), and possibly qualitative B cell defects. Hematologic cancer patients who survived
312 had higher CD8 T cell count (**Fig. 4j**), which was not seen in solid cancer patients (**Extended**
313 **Data Fig. 9b**). Conversely, CD4 T cell counts were not associated with mortality, and higher B
314 cell counts were associated with increased mortality (**Extended Data Fig. 9b, Fig 4j**). Thus,
315 patients with hematologic cancers, in the setting of defective humoral immunity, were more
316 highly dependent on adequate CD8 T cell counts than patients with solid cancers. Finally,
317 Classification and Regression Tree Analysis (CART) identified a CD8 T cell level that was
318 predictive of survival after COVID-19 in patients with hematologic cancers (**Fig. 4k**). Taken
319 together, these findings suggest that CD8 T cells are critical for anti-viral immunity in
320 hematologic malignancy patients and may at least partially mitigate the negative impact of B-cell
321 depletion on COVID outcomes.

322

323 Discussion

324 A notable feature of the COVID-19 pandemic has been the dramatic heterogeneity in clinical
325 presentations and outcomes, yet mechanistic explanations for the wide variance in disease
326 severity have remained elusive. Early on, acute phase reactants and systemic cytokines were
327 implicated in patient outcomes⁴⁶ and hospital stay and mortality were decreased by
328 dexamethasone⁴⁷, suggesting that an excessive host immune response might contribute to
329 COVID-19 mortality. However, there were also indications that inadequate host immunity might
330 contribute to adverse COVID-19 outcomes, including the association of lymphopenia with
331 mortality as well as the potentially inferior outcomes of patients on chronic immunosuppression,
332 such as patients with autoimmune diseases or organ transplant recipients⁴⁸⁻⁵¹. Recent studies
333 defined immune signatures associated with severe COVID-19, including activated CD4, CD8 T
334 cells, plasmablasts, and robust antibody responses^{15, 16, 20, 52}. Nevertheless, the individual roles
335 of these cell types in acute COVID-19 remained unclear. We speculated that investigating both
336 the clinical outcomes and immunologic profile of cancer patients might shed valuable insight into
337 how arms of the immune system contribute to viral control and mortality during COVID-19.
338 Immune investigation in hematologic malignancies is especially relevant because the disease
339 directly impacts the lymphoid and myeloid immune cells, and is commonly treated with
340 myelosuppressive and B cell-depleting therapies including CD20 targeting antibodies.

341 Our investigation reveals several novel findings. First, we establish in a prospective
342 clinical cohort that hematologic malignancy is an independent predictor of COVID-19 mortality
343 after adjusting for ECOG performance and disease status. We observed a higher mortality rate
344 in patients with hematologic (53%) versus solid cancers (34%), which were substantially higher
345 than in the general population (2.7%)²⁸. The high mortality rates for hematologic cancer in this
346 study were consistent with a recent meta-analysis of 2,361 hospitalized patients with
347 hematologic cancer (40%)⁵³. This finding highlights the importance of transmission mitigation

348 efforts for this vulnerable population⁵⁴. Furthermore, we demonstrate that excess mortality
349 observed with hematologic cancers persisted (HR 2.5) after adjustment for independent
350 predictors of cancer mortality, including age, smoking history, poor performance status, and
351 active or advanced disease. Adjustment for these factors was necessary to determine that the
352 increased mortality difference seen in hematologic cancer was in fact, driven by cancer subtype,
353 rather than differences in patient characteristics. These data can better inform hospitalized
354 patients with hematologic cancers of their expected outcomes, irrespective of performance
355 status or active cancer status, thereby improving decision-making between best supportive care
356 or aggressive interventions. The disease-specific increased risk of COVID-19 associated
357 mortality in hematologic cancer patients may also influence the prioritization and distribution of
358 vaccinations to this very high-risk population.

359 Second, using high dimensional analyses, we define immune phenotypes associated
360 with mortality during COVID-19. In particular, we identify the immune phenotype that drives the
361 mortality difference between solid and liquid malignancy. A balanced immunity that included
362 CD4, CD8, and B cells responses (phenotypes 2 and 4b) was associated with low mortality. In
363 contrast, an immune signature with robust B cell and humoral responses, but absent T cell
364 responses (phenotype 5), was associated with the highest mortality (>60%). A high mortality for
365 patients with immune phenotype 5 was consistent in both the Penn and MSKCC cohorts, and in
366 patients with solid cancer, hematologic cancer, and infected patients without cancer. Thus,
367 humoral immunity alone is often not sufficient in acute COVID-19. In fact, greater B cell
368 responses was associated with higher mortality in both solid and liquid cancer. B cell responses
369 may be a marker of disease severity, as seen with plasmablasts^{15, 20} and neutrophils^{20, 55, 56} in
370 severe COVID-19. Alternatively, some components of the B cell and humoral responses may be
371 aberrant and pathogenic, as may be the case with autoantibodies targeting type I interferons in
372 severe COVID-19⁵⁷.

373 Consistent with recent data⁵⁸, patients with solid cancers had a similar cellular immune

374 landscape and SARS-CoV-2-specific IgG responses as compared to patients without cancer.
375 Patients with hematologic cancers, however, had substantial defects in B cells and humoral
376 immunity. These defects were associated with a high mortality of 45%, as compared to 25% in
377 solid cancers. This difference in survival was driven by immune phenotype 4, which was
378 characterized by robust CD4 T cell responses in conjunction with a diminished, but not absent
379 CD8 T response. This phenotype (phenotype 4B), in the setting of preserved B cells seen in
380 solid cancer patients, was associated with a low mortality of 9%. However, this phenotype in the
381 setting of depleted B cells (phenotype 4A) seen in liquid cancer patients, was associated with a
382 mortality of 61%. This highlights the fact that CD8 T cell responses that are normally sufficient
383 may no longer be adequate in the setting of compromised humoral immunity. Thus, CD4 or B
384 cells responses, in the absence of an intact CD8 T cell response, may not be sufficient to
385 control an acute SARS-CoV-2 infection. This is reminiscent of published data demonstrating
386 that uncoordinated immune responses in the elderly was associated with severe disease and
387 poor outcomes⁵⁹.

388 Finally, by leveraging a population of COVID-19 patients in the setting of B cell depletion
389 (anti-CD20), we uncovered a critical protective role for CD8 T-cell responses. CD8 T cells are
390 known to be critical for viral clearance, particularly in response to higher viral inocula⁶⁰. Recent
391 data from transgenic mouse models show that both CD4 and CD8 T cells are necessary for
392 optimal viral clearance of SARS-CoV-2⁶¹. In patients treated with anti-CD20, absolute CD8 T
393 cell count, but not CD4 counts, was associated with survival from COVID-19 and lower viral
394 load. Although conclusions are limited by sample size, these data suggest that CD8 T cells play
395 a key role in limiting SARS-CoV-2, even in the absence of humoral immunity. Indeed, SARS-
396 CoV-2-specific CD8 T cell responses have been identified in acute and convalescent
397 individuals^{59, 62-65}. Further, in our cohort, absolute CD8 counts were predictive of outcomes in
398 the broader cohort of patients with hematologic malignancy. The compensatory role of CD8 T
399 cells was restricted to patients with hematologic, but not solid, malignancies. Thus, CD8 T cells

400 likely play an important role in the setting of quantitative and qualitative B cell dysfunction in
401 patients with lymphoma, multiple myeloma, and leukemia, undergoing anti-CD20,
402 chemotherapy, or Bruton tyrosine kinase (BTK) inhibition. CD8 T cell counts may inform on the
403 need for closer monitoring and a lower threshold for hospitalization in COVID-19 patients with
404 hematologic malignancies. Furthermore, the clinical benefit of dexamethasone, which
405 demonstrated an overall mortality benefit in hospitalized COVID-19+ patients but is known to
406 suppress CD8 T cell responses⁶⁶, should be investigated further in patients who recently
407 received anti-CD20 therapy.

408 Recent analysis demonstrated that patients treated with B-cell depleting agents had the
409 highest mortality rate, although this analysis did not account for whether the risk was modulated
410 by CD8 count. Our findings do not exclude the possibility that B-cell depleting therapies may be
411 associated with adverse outcomes in this population but rather extend these findings to suggest
412 that an adequate CD8-dependent T cell response is essential for patients in whom humoral
413 immunity is compromised. We did, however, observe a profound depletion of both naive CD4
414 and CD8 T cells in patients receiving B-cell depleting agents. Naive T-cells, and particularly
415 naive CD4 T cells, are known to require tonic TCR signaling driven by APC-presented self-
416 antigens for persistence^{67, 68}. We speculate that depletion of functional B cells, particularly in the
417 context of B cell depleting therapy, might lead to concomitant naive T cell depletion and a
418 corresponding increase in the effector and activated CD8 T cells. Although the clinical relevance
419 of naive T cell depletion in the setting of anti-CD20 is still unclear - it is notable that depletion of
420 naive T cells in the elderly was associated with increased disease severity and poor
421 outcomes⁵⁹.

422 Importantly, both B-cell depleting therapies and cytotoxic chemotherapy agents which
423 can compromise the T-cell compartment are mainstays of lymphoma therapy. Both are
424 administered, often in combination, with curative intent for patients with aggressive lymphomas,

425 but also for debulking or palliation in patients with indolent lymphomas. Based on our data, we
426 would suggest that oncologists and patients considering treatment regimens that combine B cell
427 depletion with cytotoxic agents carefully weigh the associated increased risk of immune
428 dysregulation against the benefit of disease control when making an educated decision on
429 whether to initiate such treatments, particularly in non-curative settings.

430 Finally, our finding that CD8 T cell immunity is critical for survival in hematologic
431 malignancy patients with COVID-19 has profound implications for the vaccination of these
432 patients. Both the Pfizer and Moderna vaccines, as well as the Johnson and Johnson vaccine
433 currently under investigation, induce robust CD8 T cell responses in addition to humoral
434 responses⁶⁹⁻⁷¹. Our findings suggest that vaccination of hematologic patients might enhance the
435 protective capacity of CD8 T-cells despite the likely absence of a humoral response. We are
436 conducting ongoing studies to monitor the immune profile of patients undergoing vaccination
437 prospectively to determine if this is the case. Ultimately, understanding how the immune
438 response relates to disease severity, cancer type, and cancer treatment will provide important
439 insight into the pathogenesis of and protective immunity from SARS-CoV-2, which may have
440 implications for the development and prioritization of therapeutics and vaccines in cancer
441 subpopulations.

442

443

444

445

446

447

448

449

450 **Methods:**

451 **COVID-19 Outcomes in Patients with Cancer, COPE**

452 General Design/Patient Selection

453 We conducted a prospective cohort study of patients with cancer hospitalized with
454 COVID-19 (UPCC 06920). Informed consent was obtained from all patients. Adult patients with
455 a current or prior diagnosis of cancer and hospitalized with a probable or confirmed diagnosis of
456 COVID-19, as defined by the WHO criteria⁷², within the University of Pennsylvania Health
457 System (UPHS) between April 28, 2020 and September 15, 2020 were approached for consent.
458 Participating hospitals included the Hospital of the University of Pennsylvania, Presbyterian
459 Hospital, Pennsylvania Hospital, and Lancaster General Hospital. The index date was defined
460 as the first date of hospitalization within the health system for probable or confirmed COVID-19.
461 Repeat hospitalizations within 7 days of discharge were considered within the index admission.
462 Patients who died prior to being approached for consent were retrospectively enrolled. Patients
463 were followed from the index date to 30-days following their discharge or until death by any
464 cause. This study was approved by the institutional review boards of all participating sites.

465 Data Collection

466 Baseline characteristics including patient (age, gender, race/ethnicity, comorbidities,
467 smoking history, body mass index) and cancer (tumor type, most recent treatment, ECOG
468 performance status, active cancer status) factors as well as COVID-19 related clinical factors
469 including change in levels of care, complications, treatments such as need for mechanical
470 ventilation, laboratory values (complete blood counts with differentials and inflammatory
471 markers including LDH, CRP, ferritin, and IL-6), and final disposition were extracted by trained
472 research personnel using standardized abstraction protocols. Active cancer status was defined
473 by diagnosis or treatment within 6 months of admission date. Cancer treatment status was
474 determined by the most recent treatment within 3 months prior to admission date.

475 The primary study endpoint was all-cause mortality within 30-days of hospital discharge.
476 Disease severity was categorized using the NIH ordinal scale including all post-hospitalization
477 categories: 1, hospitalized, not requiring supplemental oxygen but requiring ongoing medical
478 care; 2, hospitalized requiring any supplemental oxygen; 3, hospitalized requiring noninvasive
479 mechanical ventilation or use of high-flow oxygen devices; 4, hospitalized receiving invasive
480 mechanical ventilation or extracorporeal membrane oxygenation (ECMO); 5, death⁷³, and was
481 assessed every 7 days throughout a patient's admission.

482 Statistical Analysis

483 Cohort characteristics were compared using standard descriptive statistics. One-time
484 imputation of missing values for ECOG was done using the predicted mean value from an
485 ordinal logistic model (proportional odds) of complete data. The ordinal model was fitted with
486 forward stepwise selection, with entry at $p=0.1$ and removal at 0.2, using clinical variables
487 expected to be correlated with ECOG performance status. Those variables included several
488 items in the Charlson and severity score, and other clinical variables.

489 Univariate analyses examined demographic and clinical variables and cancer subtype
490 (hematologic versus solid cancer) as predictors of death within 30 days of discharge and of ICU
491 admission. Odds ratios and 95% CIs were used to generate the forest plot illustration. Baseline
492 laboratory tests were compared by cancer type using Mann-Whitney tests and available RT-
493 PCR data was used to determine length of RT-PCR positivity by cancer type.

494 Rates of ICU admission and death were calculated for the overall cohort and
495 stratified by cancer subtype. A multivariate logistic model was used to examine the
496 adjusted effect of solid versus hematologic designation. Covariates included
497 demographic variables of age and sex (race was omitted for missing data). Covariates
498 also included clinical variables that attained a p -value of 0.1 in the univariate analyses.
499 The final model included age, sex, smoking status, active disease status, and ECOG

500 performance status. A cox proportional hazards regression model was also performed
501 to determine the association between cancer type and mortality and identically adjusted
502 for age, sex, smoking status, active cancer status, and ECOG performance
503 status. Overall survival (OS) was measured from date of hospitalization to last follow up
504 or death and the median OS was estimated using Kaplan-Meier method and differences
505 by cancer subtype compared using log-rank test.

506

507 **Immune profiling of patients hospitalized for COVID-19, MESSI**

508 Information on clinical cohort, sample processing, and flow cytometry is described in Mathew et
509 al, Science 2020. Briefly, Patients admitted to the Hospital of the University of Pennsylvania with
510 a positive SARS-CoV-2 PCR test were screened and approached for informed consent within 3
511 days of hospitalization. Peripheral blood was collected from all subjects and clinical data were
512 abstracted from the electronic medical record into standardized case report forms. All
513 participants or their surrogates provided informed consent in accordance with protocols
514 approved by the regional ethical research boards and the Declaration of Helsinki. Methods for
515 PBMC processing, flow cytometry, and antibodies used were previously described¹⁵.

516

517 **Serologic enzyme-linked immunosorbent assay (ELISA)**

518 ELISAs were completed using plates coated with the receptor binding domain (RBD) of
519 the SARS-CoV-2 spike protein as previously described⁴⁴. Briefly, Prior to testing, plasma and
520 serum samples were heat-inactivated at 56°C for 1 hour. Plates were read at an optical density
521 (OD) of 450nm using the SpectraMax 190 microplate reader (Molecular Devices). Background
522 OD values from the plates coated with PBS were subtracted from the OD values from plates
523 coated with recombinant protein. Each plate included serial dilutions of the IgG monoclonal
524 antibody CR3022, which is reactive to the SARS-CoV-2 spike protein, as a positive control to

525 adjust for inter assay variability. Plasma and serum antibody concentrations were reported as
526 arbitrary units relative to the CR3022 monoclonal antibody. A cutoff of 0.48 arbitrary units was
527 established from a 2019 cohort of pre-pandemic individuals and used for defining seropositivity.

528

529 **Flow Cytometry and statistical analysis**

530 Samples were acquired on a 5 laser BD FACS Symphony A5. Standardized SPHERO
531 rainbow beads (Spherotech, Cat#RFP-30-5A) were used to track and adjust PMTs over time.
532 UltraComp eBeads (ThermoFisher, Cat#01-2222-42) were used for compensation. Up to $2 \times$
533 10^6 live PBMC were acquired per each sample. During the early sample acquisition period,
534 three antibodies in the flow panel were changed. Three cancer patients and twelve non-cancer
535 patients were stained using this earlier flow panel. Flow features of these patients were visually
536 assessed for batch variations against data from the later flow panel. The three cancer patients
537 were included with the rest of the cohort when batch effects were determined to have little
538 impact on confidence in gated populations. These three cancer patients were excluded in
539 analysis of cell populations defined by proteins associated with the three changed antibodies.

540 Due to the heterogeneity of clinical and flow cytometric data, non-parametric tests of
541 association were preferentially used throughout the study. Tests of association between mixed
542 continuous variables versus non-ordered categorical variables ($n=2$) were performed by Mann-
543 Whitney test. Tests of association between binary variables versus non-ordered categorical
544 variables ($n=2$) were performed using Pearson Chi Square test. All tests were performed using
545 a nominal significance threshold of $P < 0.05$ with Prism version 9 (GraphPad Software) and Excel
546 (Microsoft Office Suite). Classification and Regression Tree analysis (CART) was performed
547 using R package 'rpart'.

548

549

550 **High dimensional data analysis of flow cytometry data**

551 UMAP analyses were conducted using R package *uwot*. FlowSOM analyses were
552 performed on Cytobank (<https://cytobank.org>). Lymphocytes and non-naive CD8 T cells were
553 analyzed separately. An artifact due to monocyte contamination was removed from the FCS as
554 defined by high CD16 and side scatter area (SSC-A). UMAP analysis was performed using
555 equal down sampling of 10000 cells from each FCS file in lymphocytes and 1500 cells in non-
556 naive CD8 T cells, with a nearest neighbors of 15, minimum distance of 0.01, number of
557 components of 2, and a euclidean metric. The FCS files were then fed into the FlowSOM
558 clustering algorithm. A new self-organizing map (SOM) was generated for both lymphocytes and
559 non-naive CD8 using hierarchical consensus clustering. For each SOM, 225 clusters and 10
560 metaclusters were identified. For lymphocytes, the following markers were used in the UMAP
561 and FlowSOM analysis: CD45RA, PD-1, IgD, CXCR5, CD8, CD19, CD3, CD16, CD138,
562 Eomes, TCF-1, CD38, CD95, CCR7, CD21, Ki-67, CD27, CD4, CX3CR1, CD39, T-bet, HLA-
563 DR, and CD20. For non-naive CD8 T cells, the following markers were used: CD45RA, PD-1,
564 CXCR5, CD16, Eomes, TCF-1, CD38, CCR7, Ki-67, CD27, CX3CR1, CD39, T-bet, and HLA-
565 DR. For FlowSOM analysis of non-naive CD8 T cells, two patients at day seven without data
566 from day zero were included. Heatmaps were visualized using R function *heatmap*.

567 To group individuals based on lymphocyte landscape, pairwise Earth Mover's Distance
568 (EMD) value was calculated on the lymphocyte UMAP axes using the *emd* package in R.
569 Resulting scores were hierarchically clustered using the *hclust* package in R.

570

571 **Immune profiling of patients hospitalized for COVID-19, MSKCC**

572 Patients admitted to Memorial Sloan Kettering Cancer Center with a positive SARS-CoV-2 PCR
573 test were eligible for inclusion. For inpatients, clinical data were abstracted from the electronic
574 medical record into standardized case report forms. Clinical laboratory data were abstracted
575 from the date closest to research blood collection. Peripheral blood was collected into BD
576 Horizon Dri tubes (BD, Cat#625642). Immunophenotyping of peripheral blood mononuclear

577 cells via flow cytometry was performed in the MSKCC clinical laboratory. The lymphocyte panel
578 included CD45 FITC (BD, 340664, clone 2D1), CD56+16 PE (BD 340705, clone B73.1; BD
579 340724, clone NCAM 16.2), CD4 PerCP-Cy5.5 (BD 341653, clone SK3), CD45RA PC7 (BD
580 649457, clone L48), CD19 APC (BD 340722, clone SJ25C1), CD8 APC-H7 (BD 641409, clone
581 SK1), and CD3 BV 421 (BD 562426, clone UCHT1). The naive/effector T panel included CD45
582 FITC (BD 340664, clone 2D1), CCR7 PE (BD 560765, clone 150503), CD4 PerCP-Cy5.5 (BD
583 341653, clone SK3), CD38 APC (BioLegend, 303510, clone HIT2), HLA-DR V500 (BD 561224,
584 clone G46-6), CD45RA PC7 (BD 649457, clone L48), CD8 APC-H7 (BD 641409, clone SK1),
585 and CD3 BV 421 (BD 562426, clone UCHT1). The immune phenotypes were based on NIH
586 vaccine consensus panels and the Human Immunology Project⁷⁴. Samples were acquired on a
587 BD FACS Canto using FACSDiva software.

588

589 **Data Availability Statement:** Flow Cytometry data collected in this study was deposited to the
590 Human Pancreas Analysis Program (HPAP-RRID:SCR_016202) Database and Cytobank62
591

592 **Funding**

593 ACH was funded by grant CA230157 from the NIH. NJM was supported by NIH HL137006,
594 HL137915. DM was funded by T32 CA009140. JRG is a Cancer Research Institute-Mark
595 Foundation Fellow. ALG was supported by the Leukemia and Lymphoma Society Scholar in
596 Clinical Research Award. JRG, JEW, CA, ACH, and EJW are supported by the Parker Institute
597 for Cancer Immunotherapy which supports the Cancer Immunology program at the University of
598 Pennsylvania. E.J.W. was supported by NIH grants AI155577, AI112521, AI082630, AI201085,
599 AI123539, AI117950 and funding from the Allen Institute for Immunology to E.J.W. SV is
600 supported by funding from the Pershing Square Sohn Cancer Research Foundation. SV is a
601 consultant from Immunai and ADC therapeutics. ACH is a consultant for Immunai. RHV reports
602 having received consulting fees from Medimmune and Verastem; and research funding from
603 Fibrogen, Janssen, and Lilly. He is an inventor on a licensed patents relating to cancer cellular
604 immunotherapy and cancer vaccines, and receives royalties from Children's Hospital Boston for
605 a licensed research-only monoclonal antibody. JW is serving as a consultant for Adaptive
606 Biotechnologies, Advaxis, Amgen, Apricity, Array BioPharma, Ascentage Pharma, Astellas,
607 Bayer, BeiGene, Bristol-Myers Squibb, Celgene, Chugai, Elucida, Eli Lilly, F-Star, Genentech,
608 Imvaq, Janssen, Kyowa Hakko Kirin, Kleo Pharmaceuticals, Linnaeus, MedImmune, Merck,
609 Neon Therapeutics, Northern Biologics, Ono, Polaris Pharma, Polynoma, PsiOxus, PureTech,
610 Recepta, Takara Bio, Trieza, Sellas Life Sciences, Seramatrix, Surface Oncology, Syndax and
611 Synthologic. JW received research support from Bristol-Myers Squibb, MedImmune, Merck and
612 Genentech and has equity in Potenza Therapeutics, Tizona Pharmaceuticals, Adaptive
613 Biotechnologies, Elucida, Imvaq, BeiGene, Trieza and Linnaeus.

614

615 **Author contributions**

616 ACH, RM, SV, and EMB conceived the project; ACH, SV, NAH designed all experiments. ACH,
617 RM, EMB, AMD, IPM conceived the PENN COPE cohort. EMB, JR, FP, OO, KN, CZ, MG,
618 ARW, CAGI, EMK, CR, KRB, ST, and CW enrolled patients and collected data for COPE. EMB,
619 RM, AMD, and ACH designed data and statistical analysis for COPE. PW performed statistical
620 analysis for COPE. NJM conceived the PENN MESSI-COVID clinical cohort, ARW, CAGI, OO,
621 RSA, TGD, TJ, HMG, JPR, and NJM enrolled patients and collected data for MESSI-
622 COVID. NAH, AEB, and JYK performed downstream flow cytometry analysis for MESSI-
623 COVID. SG, MEW, CMM, SEH analyzed COVID-19 patient plasma and provided antibody data.
624 NAH, JRG, ARG, CA, DAO performed computational and statistical analyses. CA compiled and
625 JRG, DO, and CA analyzed clinical metadata for MESSI-COVID.
626 SV and JW conceived the MSKCC cohort. SV, AK, AW, SD, and SB provided clinical samples
627 from MSKCC Cohort. PM performed downstream flow cytometry analysis. NEB performed
628 quantitative PCR experiments for COVID viral load. NAH and ACH compiled figures. KNM, LS,
629 RHV, JDW, EJW, provided intellectual input. EMB, SV, RM, and ACH wrote the manuscript; all
630 authors review the manuscript.

631

632 **Acknowledgements**

633

634 The authors thank patients and blood donors, their families and surrogates, and medical
635 personnel. In addition we thank the **UPenn COVID Processing Unit**: A unit of individuals from
636 diverse laboratories at the University of Pennsylvania who volunteered time and effort to enable
637 study of COVID-19 patients during the pandemic: Sharon Adamski, Zahidul Alam, Mary M.
638 Addison, Katelyn T. Byrne, Aditi Chandra, H  l  ne C. Descamps, Nicholas Han, Yaroslav
639 Kaminskiy, Shane C. Kammerman, Justin Kim, Allison R. Greenplate, Kurt D'Andrea, Jacob T.
640 Hamilton, Nune Markosyan, Julia Han Noll, Dalia K. Omran, Ajinkya Pattekar, Eric Perkey,
641 Elizabeth M. Prager, Dana Pueschl, Austin Rennels, Jennifer B. Shah, Jake S. Shilan, Nils
642 Wilhausen, Ashley N. Vanderbeck. All affiliated with the University of Pennsylvania Perelman
643 School of Medicine.

644

645

646

647

648

649

650

651

652

653

654

655

656

657

658 **References**

- 659 **1.** Prescott HC, Girard TD: Recovery From Severe COVID-19: Leveraging the Lessons of Survival From
660 Sepsis. *JAMA* 324:739, 2020
- 661 **2.** Wu Z, McGoogan JM: Characteristics of and Important Lessons From the Coronavirus Disease 2019
662 (COVID-19) Outbreak in China: Summary of a Report of 72 314 Cases From the Chinese Center for
663 Disease Control and Prevention [Internet]. *JAMA* , 2020[cited 2020 Mar 28] Available from:
664 <https://jamanetwork.com/journals/jama/fullarticle/2762130>
- 665 **3.** Blanco-Melo D, Nilsson-Payant BE, Liu W-C, et al: Imbalanced Host Response to SARS-CoV-2 Drives
666 Development of COVID-19. *Cell* 181:1036-1045.e9, 2020
- 667 **4.** Hadjadj J, Yatim N, Barnabei L, et al: Impaired type I interferon activity and inflammatory responses in
668 severe COVID-19 patients. *Science* 369:718–724, 2020
- 669 **5.** Arunachalam PS, Wimmers F, Mok CKP, et al: Systems biological assessment of immunity to mild
670 versus severe COVID-19 infection in humans. *Science* 369:1210–1220, 2020
- 671 **6.** Chen G, Wu D, Guo W, et al: Clinical and immunological features of severe and moderate coronavirus
672 disease 2019. *J Clin Invest* 130:2620–2629, 2020
- 673 **7.** Huang C, Wang Y, Li X, et al: Clinical features of patients infected with 2019 novel coronavirus in
674 Wuhan, China. *The Lancet* 395:497–506, 2020
- 675 **8.** Tan L, Wang Q, Zhang D, et al: Lymphopenia predicts disease severity of COVID-19: a descriptive and
676 predictive study [Internet]. *Signal Transduct Target Ther* 5, 2020[cited 2020 Oct 20] Available from:
677 <http://www.nature.com/articles/s41392-020-0148-4>
- 678 **9.** Zhao Q, Meng M, Kumar R, et al: Lymphopenia is associated with severe coronavirus disease 2019
679 (COVID-19) infections: A systemic review and meta-analysis. *Int J Infect Dis* 96:131–135, 2020
- 680 **10.** Qin C, Zhou L, Hu Z, et al: Dysregulation of Immune Response in Patients With Coronavirus 2019
681 (COVID-19) in Wuhan, China. *Clin Infect Dis* 71:762–768, 2020
- 682 **11.** Laing AG, Lorenc A, del Molino del Barrio I, et al: A dynamic COVID-19 immune signature includes
683 associations with poor prognosis. *Nat Med* 26:1623–1635, 2020
- 684 **12.** Yale IMPACT Team, Lucas C, Wong P, et al: Longitudinal analyses reveal immunological misfiring in
685 severe COVID-19. *Nature* 584:463–469, 2020
- 686 **13.** Giamarellos-Bourboulis EJ, Netea MG, Rovina N, et al: Complex Immune Dysregulation in COVID-19
687 Patients with Severe Respiratory Failure. *Cell Host Microbe* 27:992-1000.e3, 2020
- 688 **14.** Mann ER, Menon M, Knight SB, et al: Longitudinal immune profiling reveals key myeloid signatures
689 associated with COVID-19. *Sci Immunol* 5:eabd6197, 2020
- 690 **15.** Mathew D, Giles JR, Baxter AE, et al: Deep immune profiling of COVID-19 patients reveals distinct
691 immunotypes with therapeutic implications. *Science* 369:eabc8511, 2020

- 692 **16.** Su Y, Chen D, Yuan D, et al: Multi-Omics Resolves a Sharp Disease-State Shift between Mild and
693 Moderate COVID-19. *Cell* 183:1479-1495.e20, 2020
- 694 **17.** De Biasi S, Meschiari M, Gibellini L, et al: Marked T cell activation, senescence, exhaustion and
695 skewing towards TH17 in patients with COVID-19 pneumonia [Internet]. *Nat Commun* 11, 2020[cited
696 2020 Dec 22] Available from: <http://www.nature.com/articles/s41467-020-17292-4>
- 697 **18.** Zheng H-Y, Zhang M, Yang C-X, et al: Elevated exhaustion levels and reduced functional diversity of T
698 cells in peripheral blood may predict severe progression in COVID-19 patients. *Cell Mol Immunol*
699 17:541–543, 2020
- 700 **19.** Xu Z, Shi L, Wang Y, et al: Pathological findings of COVID-19 associated with acute respiratory
701 distress syndrome. *Lancet Respir Med* , 2020
- 702 **20.** Kuri-Cervantes L, Pampena MB, Meng W, et al: Comprehensive mapping of immune perturbations
703 associated with severe COVID-19. *Sci Immunol* 5:eabd7114, 2020
- 704 **21.** Zhao J, Yuan Q, Wang H, et al: Antibody Responses to SARS-CoV-2 in Patients With Novel
705 Coronavirus Disease 2019. *Clin Infect Dis* 71:2027–2034, 2020
- 706 **22.** Long Q-X, Liu B-Z, Deng H-J, et al: Antibody responses to SARS-CoV-2 in patients with COVID-19. *Nat*
707 *Med* 26:845–848, 2020
- 708 **23.** Ruge M, Zorzi M, Guzzinati S: SARS-CoV-2 infection in the Italian Veneto region: adverse outcomes
709 in patients with cancer. *Nat Cancer* 1:784–788, 2020
- 710 **24.** Assaad S, Avrillon V, Fournier M-L, et al: High mortality rate in cancer patients with symptoms of
711 COVID-19 with or without detectable SARS-COV-2 on RT-PCR. *Eur J Cancer* 135:251–259, 2020
- 712 **25.** Miyashita H, Kuno T: Prognosis of coronavirus disease 2019 (COVID-19) in patients with HIV infection
713 in New York City [Internet]. *HIV Med* , 2020[cited 2020 Oct 20] Available from:
714 <https://onlinelibrary.wiley.com/doi/abs/10.1111/hiv.12920>
- 715 **26.** Dai M, Liu D, Liu M, et al: Patients with cancer appear more vulnerable to SARS-COV-2: a multi-
716 center study during the COVID-19 outbreak. *Cancer Discov* CD-20-0422, 2020
- 717 **27.** Saini KS, Tagliamento M, Lambertini M, et al: Mortality in patients with cancer and coronavirus
718 disease 2019: A systematic review and pooled analysis of 52 studies. *Eur J Cancer Oxf Engl* 1990 139:43–
719 50, 2020
- 720 **28.** Coronavirus COVID-19 Global Cases [Internet], 2020[cited 2020 Oct 19] Available from:
721 <https://coronavirus.jhu.edu/map.html>
- 722 **29.** Mehta V, Goel S, Kabarriti R, et al: Case Fatality Rate of Cancer Patients with COVID-19 in a New York
723 Hospital System. *Cancer Discov* CD-20-0516, 2020
- 724 **30.** Lee LYW, Cazier J-B, Starkey T, et al: COVID-19 prevalence and mortality in patients with cancer and
725 the effect of primary tumour subtype and patient demographics: a prospective cohort study. *Lancet*
726 *Oncol* 21:1309–1316, 2020

- 727 **31.** Mato AR, Roeker LE, Lamanna N, et al: Outcomes of COVID-19 in patients with CLL: a multicenter
728 international experience. *Blood* 136:1134–1143, 2020
- 729 **32.** Chari A, Samur MK, Martinez-Lopez J, et al: Clinical features associated with COVID-19 outcome in
730 multiple myeloma: first results from the International Myeloma Society data set. *Blood* 136:3033–3040,
731 2020
- 732 **33.** Lamure S, Duléry R, Di Blasi R, et al: Determinants of outcome in Covid-19 hospitalized patients with
733 lymphoma: A retrospective multicentric cohort study. *EClinicalMedicine* 27:100549, 2020
- 734 **34.** Lee LYW, Cazier JB, Starkey T, et al: COVID-19 mortality in patients with cancer on chemotherapy or
735 other anticancer treatments: a prospective cohort study [Internet]. *The Lancet* , 2020[cited 2020 Jun 7]
736 Available from: <https://linkinghub.elsevier.com/retrieve/pii/S0140673620311739>
- 737 **35.** Albiges L, Foulon S, Bayle A, et al: Determinants of the outcomes of patients with cancer infected
738 with SARS-CoV-2: results from the Gustave Roussy cohort [Internet]. *Nat Cancer* , 2020[cited 2020 Oct
739 19] Available from: <http://www.nature.com/articles/s43018-020-00120-5>
- 740 **36.** Kuderer NM, Choueiri TK, Shah DP, et al: Clinical impact of COVID-19 on patients with cancer
741 (CCC19): a cohort study [Internet]. *The Lancet* , 2020[cited 2020 Jun 7] Available from:
742 <https://linkinghub.elsevier.com/retrieve/pii/S0140673620311879>
- 743 **37.** Garassino MC, Whisenant JG, Huang L-C, et al: COVID-19 in patients with thoracic malignancies
744 (TERAVOLT): first results of an international, registry-based, cohort study. *Lancet Oncol* 21:914–922,
745 2020
- 746 **38.** Petrilli CM, Jones SA, Yang J, et al: Factors associated with hospital admission and critical illness
747 among 5279 people with coronavirus disease 2019 in New York City: prospective cohort study. *BMJ*
748 369:m1966, 2020
- 749 **39.** Williamson EJ, Walker AJ, Bhaskaran K, et al: Factors associated with COVID-19-related death using
750 OpenSAFELY. *Nature* 584:430–436, 2020
- 751 **40.** Zhou F, Yu T, Du R, et al: Clinical course and risk factors for mortality of adult inpatients with COVID-
752 19 in Wuhan, China: a retrospective cohort study. *The Lancet* 395:1054–1062, 2020
- 753 **41.** Jee J, Foote MB, Lumish M, et al: Chemotherapy and COVID-19 Outcomes in Patients With Cancer. *J*
754 *Clin Oncol* 38:3538–3546, 2020
- 755 **42.** Robilotti EV, Babady NE, Mead PA, et al: Determinants of COVID-19 disease severity in patients with
756 cancer. *Nat Med* 26:1218–1223, 2020
- 757 **43.** Amanat F, Stadlbauer D, Strohmeier S, et al: A serological assay to detect SARS-CoV-2 seroconversion
758 in humans. *Nat Med* 26:1033–1036, 2020
- 759 **44.** Flannery DD, Gouma S, Dhudasia MB, et al: SARS-CoV-2 seroprevalence among parturient women in
760 Philadelphia. *Sci Immunol* 5:eabd5709, 2020
- 761 **45.** Orlova DY, Zimmerman N, Meehan S, et al: Earth Mover’s Distance (EMD): A True Metric for
762 Comparing Biomarker Expression Levels in Cell Populations. *PLOS ONE* 11:e0151859, 2016

- 763 **46.** Del Valle DM, Kim-Schulze S, Huang H-H, et al: An inflammatory cytokine signature predicts COVID-
764 19 severity and survival. *Nat Med* 26:1636–1643, 2020
- 765 **47.** RECOVERY Collaborative Group, Horby P, Lim WS, et al: Dexamethasone in Hospitalized Patients with
766 Covid-19 - Preliminary Report. *N Engl J Med* , 2020
- 767 **48.** Shields AM, Burns SO, Savic S, et al: COVID-19 in patients with primary and secondary
768 immunodeficiency: the United Kingdom experience. *J Allergy Clin Immunol* , 2020
- 769 **49.** Gianfrancesco M, Hyrich KL, Al-Adely S, et al: Characteristics associated with hospitalisation for
770 COVID-19 in people with rheumatic disease: data from the COVID-19 Global Rheumatology Alliance
771 physician-reported registry. *Ann Rheum Dis* 79:859–866, 2020
- 772 **50.** Pereira MR, Mohan S, Cohen DJ, et al: COVID-19 in solid organ transplant recipients: Initial report
773 from the US epicenter. *Am J Transplant Off J Am Soc Transplant Am Soc Transpl Surg* 20:1800–1808,
774 2020
- 775 **51.** Raja MA, Mendoza MA, Villavicencio A, et al: COVID-19 in solid organ transplant recipients: A
776 systematic review and meta-analysis of current literature. *Transplant Rev Orlando Fla* 35:100588, 2020
- 777 **52.** Thevarajan I, Nguyen THO, Koutsakos M, et al: Breadth of concomitant immune responses prior to
778 patient recovery: a case report of non-severe COVID-19. *Nat Med* 26:453–455, 2020
- 779 **53.** Vijenthira A, Gong IY, Fox TA, et al: Outcomes of patients with hematologic malignancies and COVID-
780 19: A systematic review and meta-analysis of 3377 patients. *Blood* , 2020
- 781 **54.** Persad G, Peek ME, Emanuel EJ: Fairly Prioritizing Groups for Access to COVID-19 Vaccines. *JAMA* ,
782 2020
- 783 **55.** Zhang B, Zhou X, Zhu C, et al: Immune Phenotyping Based on the Neutrophil-to-Lymphocyte Ratio
784 and IgG Level Predicts Disease Severity and Outcome for Patients With COVID-19. *Front Mol Biosci*
785 7:157, 2020
- 786 **56.** Liu J, Liu Y, Xiang P, et al: Neutrophil-to-lymphocyte ratio predicts critical illness patients with 2019
787 coronavirus disease in the early stage. *J Transl Med* 18:206, 2020
- 788 **57.** Bastard P, Rosen LB, Zhang Q, et al: Autoantibodies against type I IFNs in patients with life-
789 threatening COVID-19. *Science* 370, 2020
- 790 **58.** Abdul-Jawad S, Baù L, Alaguthurai T, et al: Acute immune signatures and their legacies in severe
791 acute respiratory syndrome coronavirus-2 infected cancer patients. *Cancer Cell* S1535610821000015,
792 2021
- 793 **59.** Rydyznski Moderbacher C, Ramirez SI, Dan JM, et al: Antigen-Specific Adaptive Immunity to SARS-
794 CoV-2 in Acute COVID-19 and Associations with Age and Disease Severity. *Cell* 183:996-1012.e19, 2020
- 795 **60.** Weidt G, Utermöhlen O, Zerrahn J, et al: CD8+ T lymphocyte-mediated antiviral immunity in mice as
796 a result of injection of recombinant viral proteins. *J Immunol Baltim Md* 1950 153:2554–2561, 1994
- 797 **61.** Sun J, Zhuang Z, Zheng J, et al: Generation of a Broadly Useful Model for COVID-19 Pathogenesis,
798 Vaccination, and Treatment. *Cell* 182:734-743.e5, 2020

- 799 **62.** Sekine T, Perez-Potti A, Rivera-Ballesteros O, et al: Robust T Cell Immunity in Convalescent
800 Individuals with Asymptomatic or Mild COVID-19. *Cell* 183:158-168.e14, 2020
- 801 **63.** Peng Y, Mentzer AJ, Liu G, et al: Broad and strong memory CD4+ and CD8+ T cells induced by SARS-
802 CoV-2 in UK convalescent individuals following COVID-19. *Nat Immunol* 21:1336–1345, 2020
- 803 **64.** Kared H, Redd AD, Bloch EM, et al: SARS-CoV-2-specific CD8+ T cell responses in convalescent COVID-
804 19 individuals. *J Clin Invest* , 2021
- 805 **65.** Ni L, Ye F, Cheng M-L, et al: Detection of SARS-CoV-2-Specific Humoral and Cellular Immunity in
806 COVID-19 Convalescent Individuals. *Immunity* 52:971-977.e3, 2020
- 807 **66.** Cook AM, McDonnell AM, Lake RA, et al: Dexamethasone co-medication in cancer patients
808 undergoing chemotherapy causes substantial immunomodulatory effects with implications for chemo-
809 immunotherapy strategies. *Oncoimmunology* 5:e1066062, 2016
- 810 **67.** Takeda S, Rodewald H-R, Arakawa H, et al: MHC Class II Molecules Are Not Required for Survival of
811 Newly Generated CD4+ T Cells, but Affect Their Long-Term Life Span. *Immunity* 5:217–228, 1996
- 812 **68.** Stefanová I, Dorfman JR, Germain RN: Self-recognition promotes the foreign antigen sensitivity of
813 naive T lymphocytes. *Nature* 420:429–434, 2002
- 814 **69.** Sadoff J, Le Gars M, Shukarev G, et al: Interim Results of a Phase 1-2a Trial of Ad26.COV2.S Covid-19
815 Vaccine. *N Engl J Med* , 2021
- 816 **70.** Corbett KS, Edwards DK, Leist SR, et al: SARS-CoV-2 mRNA vaccine design enabled by prototype
817 pathogen preparedness. *Nature* 586:567–571, 2020
- 818 **71.** Sahin U, Muik A, Derhovanessian E, et al: COVID-19 vaccine BNT162b1 elicits human antibody and
819 TH1 T cell responses. *Nature* 586:594–599, 2020
- 820 **72.** Global surveillance for COVID-19 caused by human infection with COVID-19 virus. [Internet]. WHO ,
821 2020 Available from: [https://apps.who.int/iris/bitstream/handle/10665/331506/WHO-2019-nCoV-](https://apps.who.int/iris/bitstream/handle/10665/331506/WHO-2019-nCoV-SurveillanceGuidance-2020.6-eng.pdf)
822 [SurveillanceGuidance-2020.6-eng.pdf](https://apps.who.int/iris/bitstream/handle/10665/331506/WHO-2019-nCoV-SurveillanceGuidance-2020.6-eng.pdf)
- 823 **73.** Beigel JH, Tomashek KM, Dodd LE, et al: Remdesivir for the Treatment of Covid-19 — Final Report. *N*
824 *Engl J Med* 383:1813–1826, 2020
- 825 **74.** Maecker HT, McCoy JP, Nussenblatt R: Standardizing immunophenotyping for the Human
826 Immunology Project. *Nat Rev Immunol* 12:191–200, 2012
- 827
- 828

Table 1 | COPE: Patient demographics and clinical characteristics.

	Total (N=100)
Age, median (IQR)	68 (57.5-77.5)
Gender, female	48 (48%)
Race	
Black	54 (54%)
White	33 (33%)
Asian	4 (4%)
Hispanic	3 (3%)
Unknown	6 (6%)
Smoking History, Ever⁺	57 (57%)
Comorbidities	
Cardiac	78 (78%)
Pulmonary	41 (41%)
Use of immunosuppressive drugs^{**}	30 (30%)
BMI, median (IQR)	26.84 (23.2-31.5)
Cancer Type	
Solid malignancy	78 (78%)
Genitourinary	19 (19%)
Breast	14 (14%)
Gastrointestinal	14 (14%)
Thoracic	9 (9%)
Other ^{***}	8 (8%)
Gynecologic	7 (7%)
Head and Neck	4 (4%)
Sarcoma	3 (3%)
Heme malignancy	22 (22%)
Lymphoma	10 (10%)
Leukemia	7 (7%)
Myeloma	3 (3%)
MDS/MPN	2 (2%)
Cancer Status, Active[#]	46 (46%)
Cancer treatment in last 3 months	
Active surveillance/surgery	53 (53%)
Cytotoxic Chemotherapy	24 (24%)
Hormone therapy	15 (15%)
Other [*]	8 (8%)
ECOG Performance Status	N=73
0-1	37 (50.7%)
2	13 (17.8%)
3-4	23 (31.5%)
⁺ Current or prior smoker ^{**} Exposure to immunosuppressive medications not including cancer treatment ^{***} Tumor types with less than 2 subjects: CNS-2, Thyroid-2, Thymus-1, Neuroendocrine-1 [#] Diagnosis or treatment within 6 months [*] Single agent immunotherapy, targeted therapy, monoclonal antibodies	

Table 2 | COPE: COVID-19 related treatment and outcomes.

	Total (N=100)	Solid (N=78)	Heme (N=22)
COVID-19 Disease Severity			
At Presentation			
No Supplemental Oxygen	35 (35.0%)	28 (35.9%)	7 (31.85)
Supplemental Oxygen	44 (44.0%)	32 (41.0%)	12 (54.6%)
Non-invasive ventilation	9 (9.00%)	7 (8.97%)	2 (9.09%)
Invasive ventilation	12 (12.0%)	11 (14.1%)	1 (4.55%)
Maximum throughout hospitalization			
No supplemental Oxygen	28 (28.0%)	24 (30.8%)	4 (18.2%)
Supplemental Oxygen	24 (24.0%)	19 (24.4%)	4 (18.2%)
Non-invasive ventilation	11 (11.0%)	8 (10.3%)	3 (13.6%)
Invasive ventilation	9 (9.00%)	9 (11.5%)	0 (0.00%)
Death	28 (28.0%)	18 (23.1%)	12 (54.5%)
COVID-19 Directed Treatment			
Steroids	51 (51.0%)	39 (50.0%)	12 (54.6%)
Remdesivir	18 (18.0%)	13 (16.7%)	5 (22.7%)
Convalescent Plasma	10 (10.0%)	6 (7.69%)	4 (18.2%)
COVID-19 Outcomes			
Thrombosis	11 (11.0%)	7 (9.09%)	4 (18.2%)
Intubation	28 (28.0%)	21 (26.9%)	7 (31.8%)
ICU admission	48 (48.0%)	37 (47.4%)	11 (50.0%)
Death	38 (38.0%)	26 (33.3%)	12 (54.6%)
Hospital Length of stay, median (IQR)	8 (4-19)	8 (4-20)	8 (4-18)

Table 3 | COPE: Event rates and point estimates of outcomes by cancer type.

	Heme	Solid
Death within 30 days of discharge		
Event rate (%)	12 (54.6%)	26 (33.3%)
Unadjusted OR (95% CI)	2.4 (0.82-7.06)	ref
Adjusted OR (95% CI) [†]	3.3 (1.01-10.8)	ref
Adjusted HR (95% CI) [†]	2.6 (1.19-5.54)	ref
[†] Logistic regression computed odds ratio (OR) and Cox regression computed hazard ratio (HR), respectively. Adjusted for age, gender, smoking status, active cancer status, and ECOG performance status.		

Fig. 1

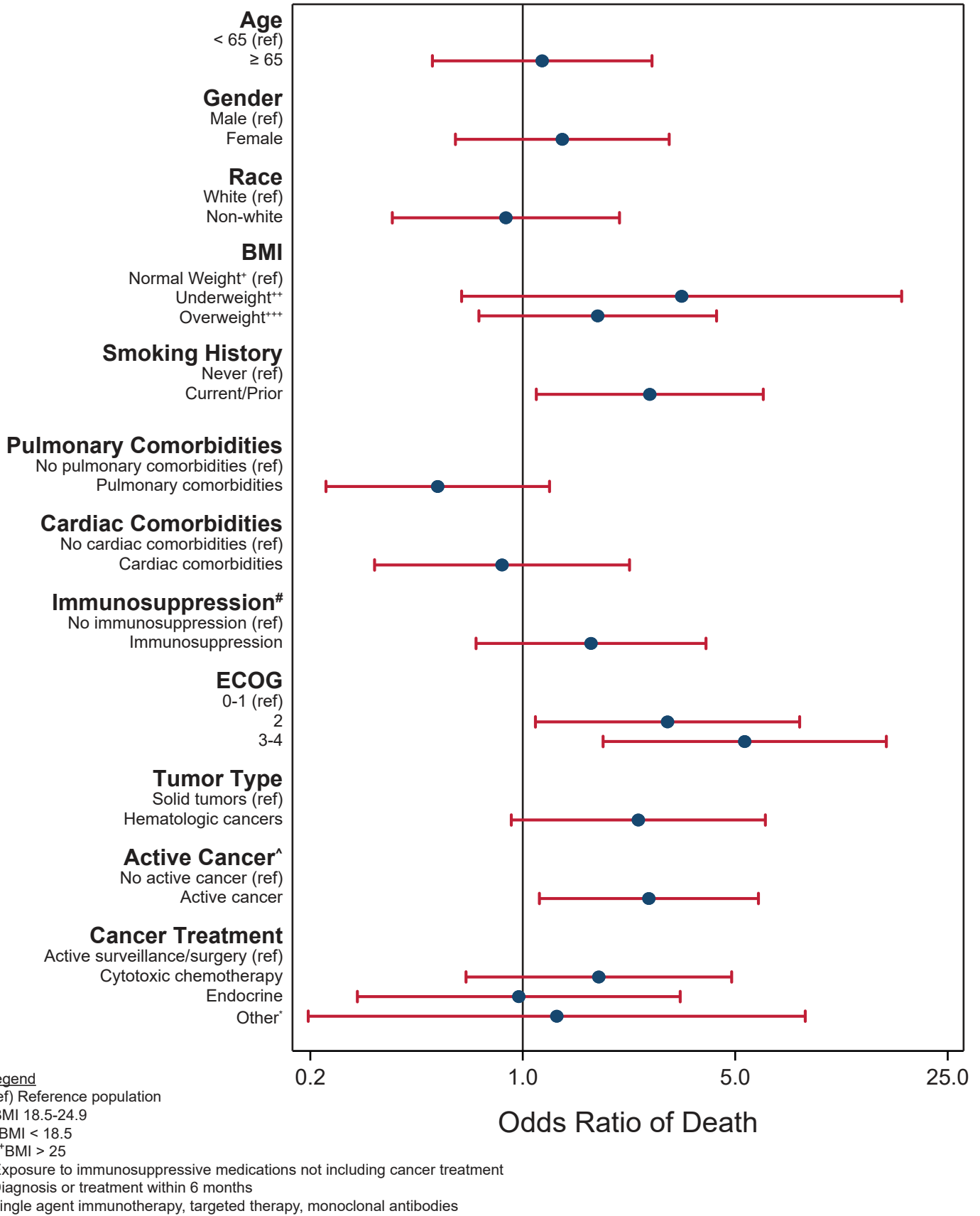


Fig. 1 | Univariate analysis of potential risk factors in COVID-19 mortality.

Fig. 2

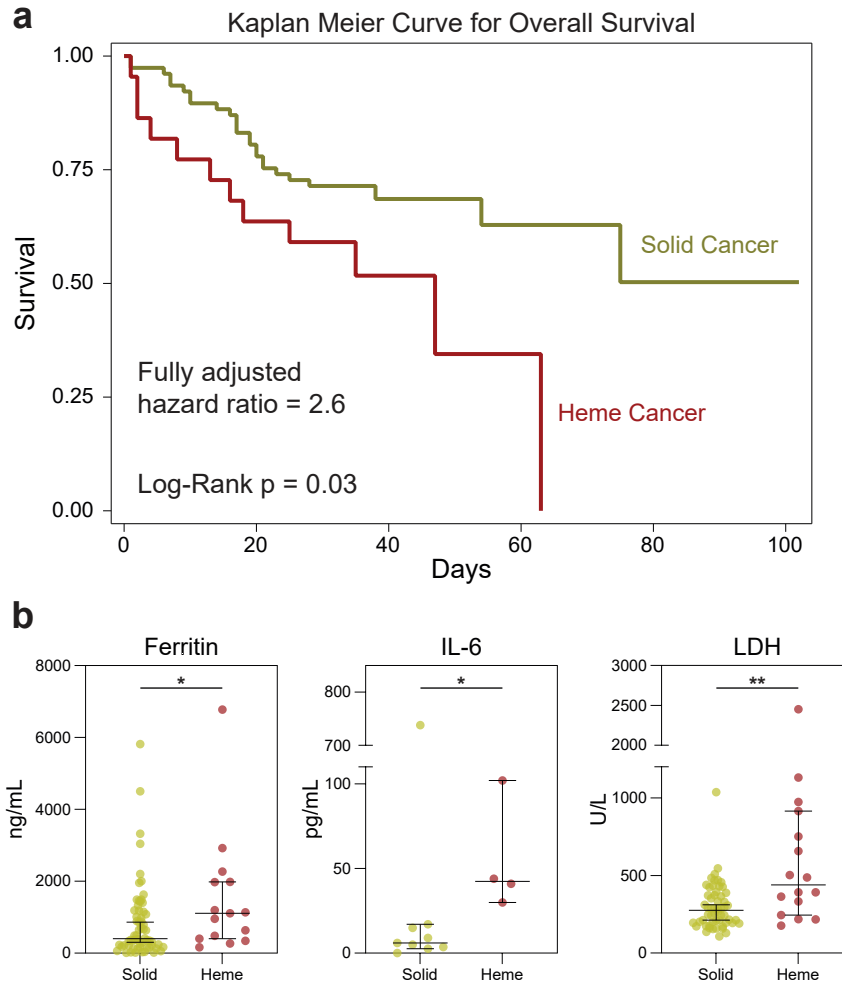


Fig. 2 | Hematologic cancer is an independent risk factor for COVID-19 related mortality. (a) Kaplan Meier curve for COVID-19 survival of patients with solid (n=77) and hematologic (n=22) cancer. Cox regression-computed hazard ratio for mortality in hematologic vs solid cancer, adjusted for age, gender, smoking status, active cancer status, and ECOG performance status. (b) Ferritin, IL-6, and LDH in solid (n=62) and hematologic (n=15) cancer hospitalized for COVID-19. (All) Significance determined by Mann Whitney test: *p<0.05, **p<0.01, ***p<0.001, and ****p<0.0001. Median and 95% CI shown.

Fig. 3

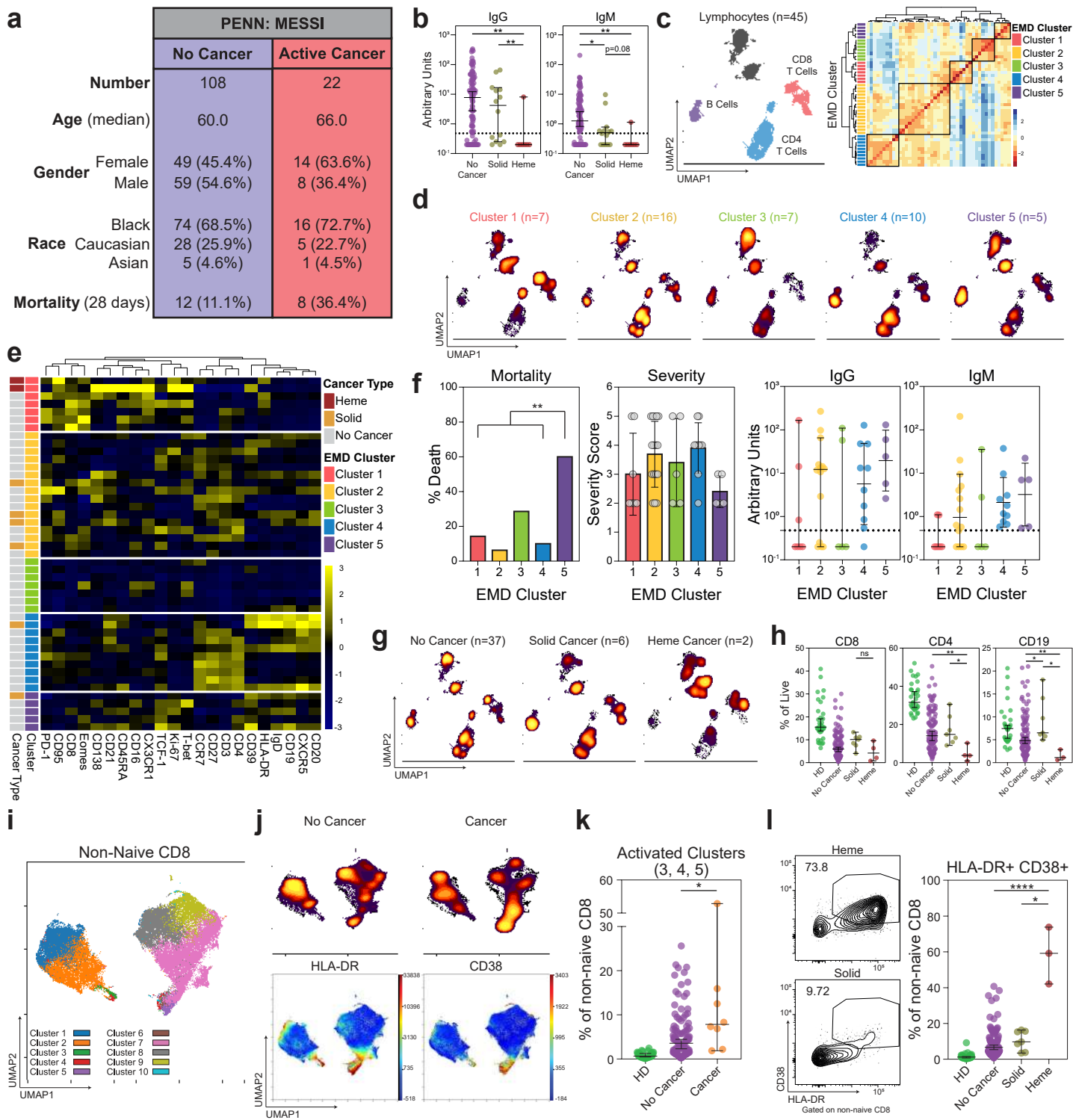


Fig. 3 | High dimensional analyses reveal immune phenotypes associated with mortality and distinct phenotypes between solid and hematologic cancers. (a) Demographic and mortality data for MESSI cohort at Penn. (b) Relative levels of SARS-CoV-2 IgG and IgM of solid (n=14) and hematologic (n=7) cancer patients and non-cancer patients (n=108). (c) (Left) Global UMAP projection of lymphocyte populations for all 45 patients pooled. (Right) Hierarchical clustering of Earth Mover's Distance (EMD) using Pearson correlation, calculated pairwise for lymphocyte populations. (d) UMAP projection of concatenated lymphocyte populations for each EMD cluster. (Yellow: High Density; Black; Low Density) (e) Heatmap showing expression patterns of various markers, stratified by EMD cluster. Heat scale calculated as column z-score of MFI. (f) Mortality, disease severity, and SARS-CoV-2 antibody data, stratified by EMD cluster (Cluster 5 n=5; Cluster 1,2,3,4 n=40). Mortality significance determined by Pearson Chi Square test. Severity assessed with NIH ordinal scale for COVID-19 clinical severity (1: Death; 8: Normal Activity)¹⁵. (g) UMAP projections of concatenated lymphocyte populations for solid cancer, hematologic cancer, and non-cancer patients. (h) CD8 and CD4 T cell and B cell frequencies in healthy donors (HD) (n=33), non-cancer (n=108), solid cancer (n=7), and heme cancer (n=4). (i) UMAP projection of non-naive CD8 T cell clusters identified by FlowSOM. (j) (Top) UMAP projections of non-naive CD8 T cells for non-cancer and cancer patients. (Bottom) UMAP projections indicating HLA-DR and CD38 protein expression on non-naive CD8 T cells for all patients pooled. (k) Frequency of activated FlowSOM clusters in HD (n=30), non-cancer (n=110), and cancer patients (n=8). (l) Representative flow plots and frequency of HLA-DR and CD38 co-expression in HD (n=30), non-cancer (n=110), solid cancer (n=7), and hematologic cancer (n=3) patients. (All) Significance determined by Mann Whitney test: *p<0.05, **p<0.01, ***p<0.001, and ****p<0.0001. Median and 95% CI shown.

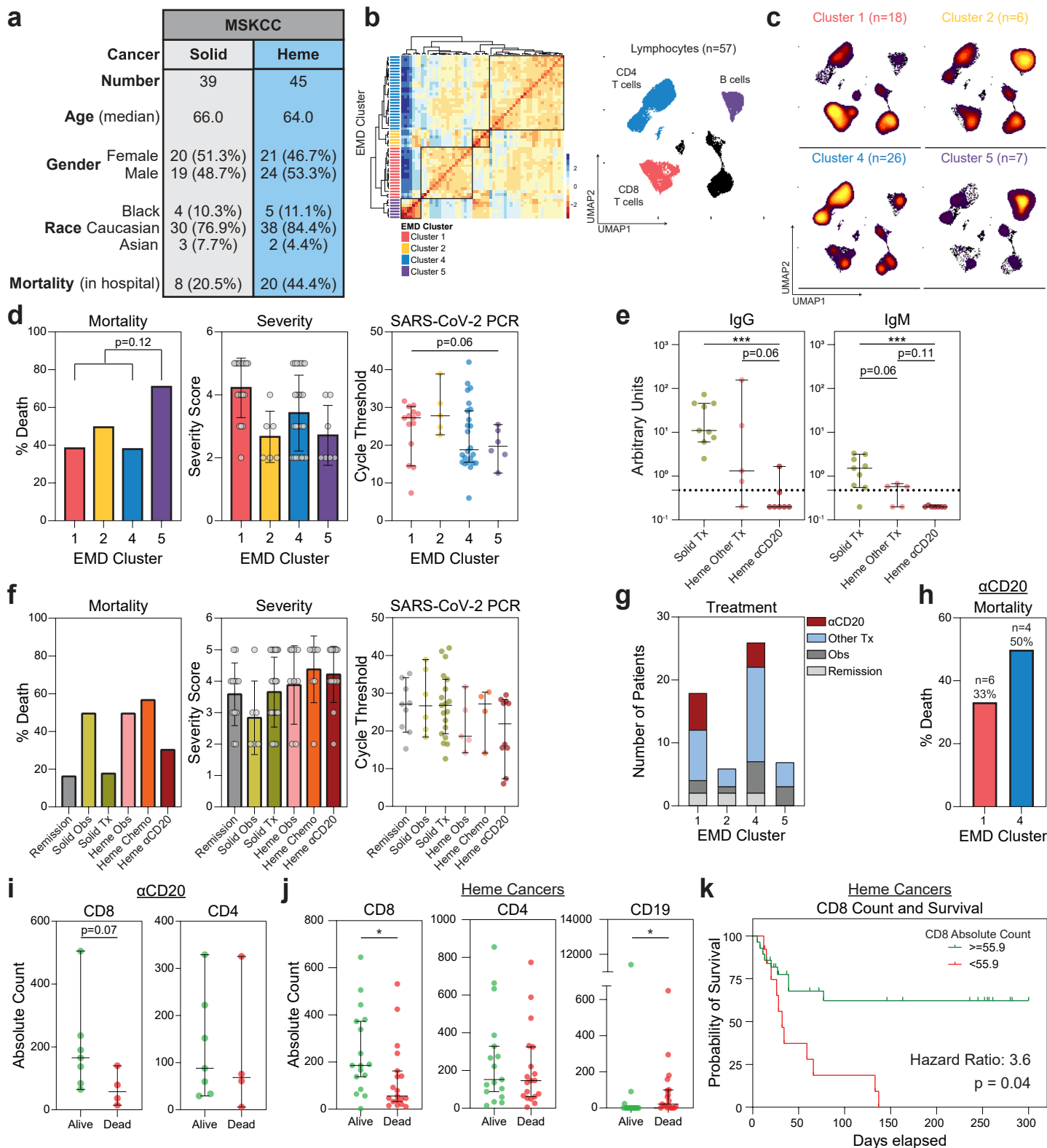
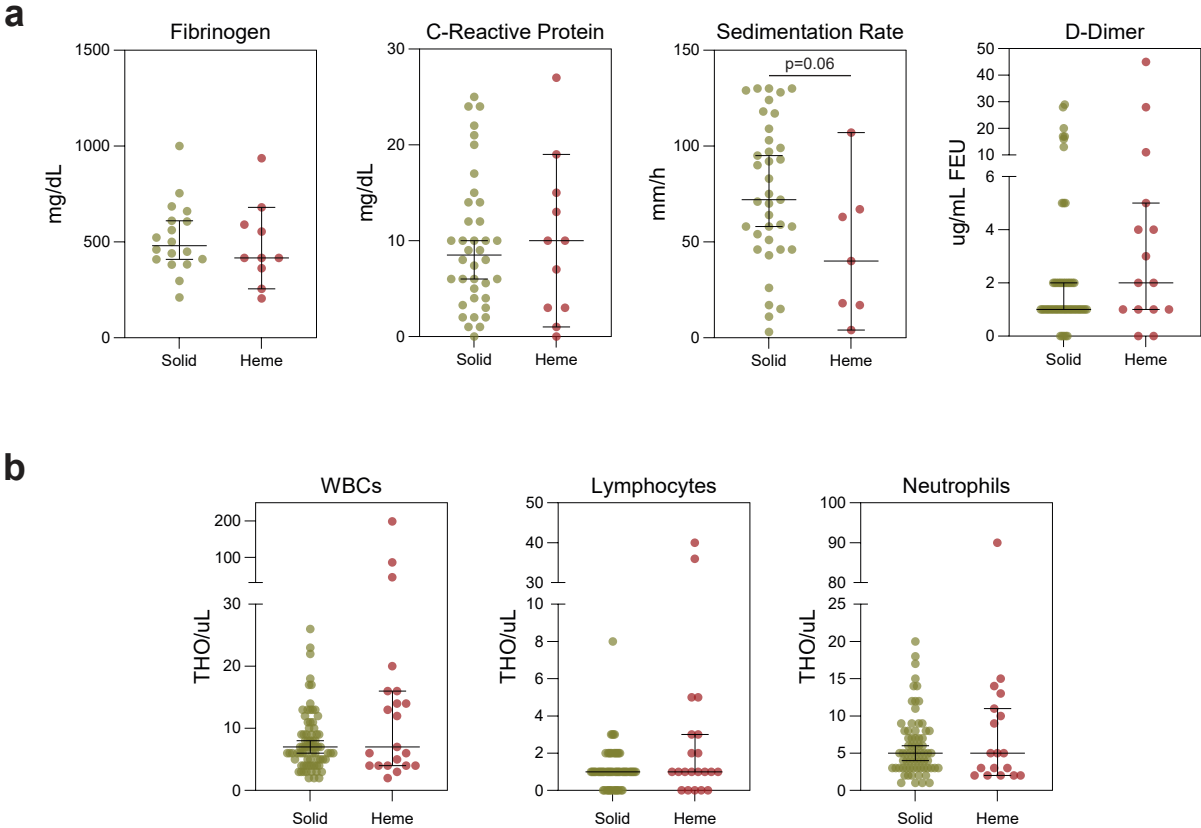
Fig. 4

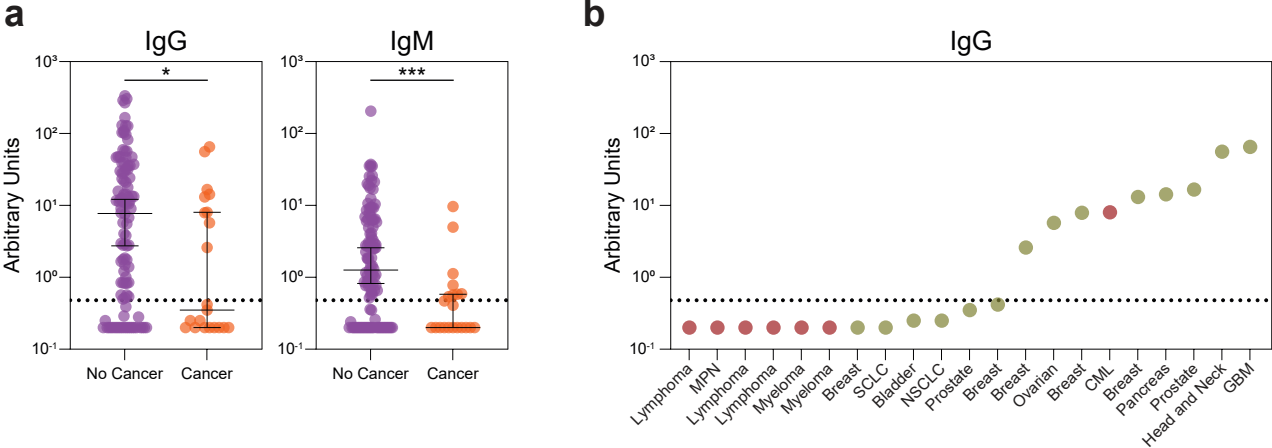
Fig. 4 | CD8 T cell counts associated with survival in hematologic cancer patients with COVID-19. (a) Demographic and mortality data of MSKCC cohort. (b) (Left) Hierarchical clustering of Earth Mover's Distance (EMD) using Pearson correlation, calculated pairwise for lymphocyte populations. (Right) Global UMAP projection of lymphocyte populations pooled. (c) UMAP projection of concatenated lymphocyte populations for each EMD cluster. (Yellow: High Density; Black: Low Density) (d) Mortality (Cluster 5 n=7; Cluster 1,2,4 n=50), severity, and RT-PCR cycle threshold (Cluster 1 n=14; Cluster 2 n=5; Cluster 4 n=24; Cluster 5 n=6) (Lower Ct: Higher viral load) stratified by EMD cluster. Mortality significance determined by Pearson Chi Square test. (e) Relative levels of SARS-CoV-2 IgG and IgM of patients with recent cancer treatments (solid tx n=9; heme αCD20 n=7; heme other tx n=5). (f) Mortality, severity, and RT-PCR cycle threshold stratified by cancer treatment (remission n=9; solid obs n=6; solid tx n=19; heme obs n=5; heme chemo n=4; heme αCD20 n=10). Severity assessed with NIH ordinal scale for COVID-19 clinical severity. (g) Recent cancer treatment of patients in each EMD cluster. (h) Mortality of patients treated with B cell depleting therapy in EMD cluster 1 (red) and EMD cluster 4 (blue). (i) Absolute CD8 and CD4 T cell counts in patients treated with B cell depleting therapy (alive n=7; dead n=4). (j) Absolute CD8 and CD4 T cell counts and B cell counts in hematologic cancer patients (alive n=17; dead n=18). (k) Kaplan-Meier curve for survival in hematologic cancer patients stratified by CD8 T cell counts (threshold = 55.9; log-rank hazard ratio) (>=55.9 n=28; <55.9 n=13). CD8 count threshold determined by Classification and Regression Tree (CART) analysis. (All) Significance determined by Mann Whitney test: *p<0.05, **p<0.01, ***p<0.001, and ****p<0.0001. Median and 95% CI shown.

Extended Data Fig. 1



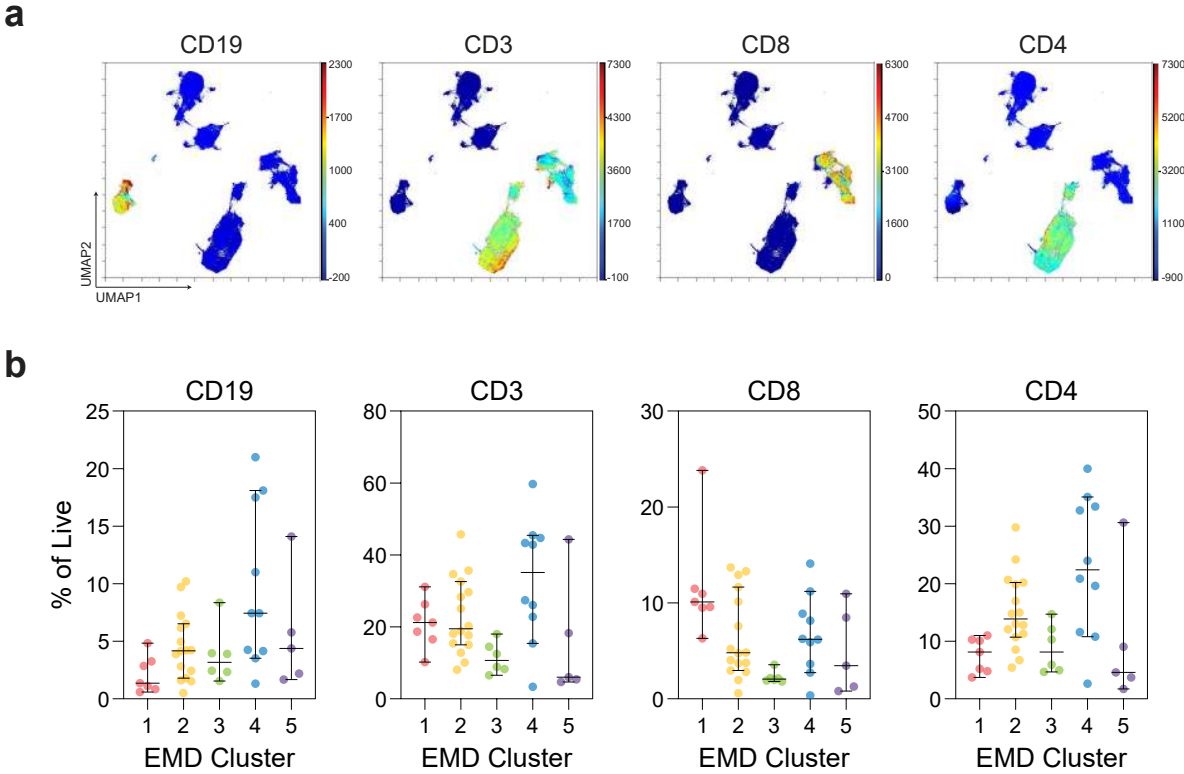
Extended Data Fig. 1 | Inflammatory markers and blood cell counts in cancer patients with COVID-19. Clinical laboratory values for (a) inflammatory markers and (b) cell counts in solid (n=62) and hematologic (n=21) cancer patients. (All) Significance determined by Mann Whitney test: *p<0.05, **p<0.01, ***p<0.001, and ****p<0.0001. Median and 95% CI shown.

Extended Data Fig. 2



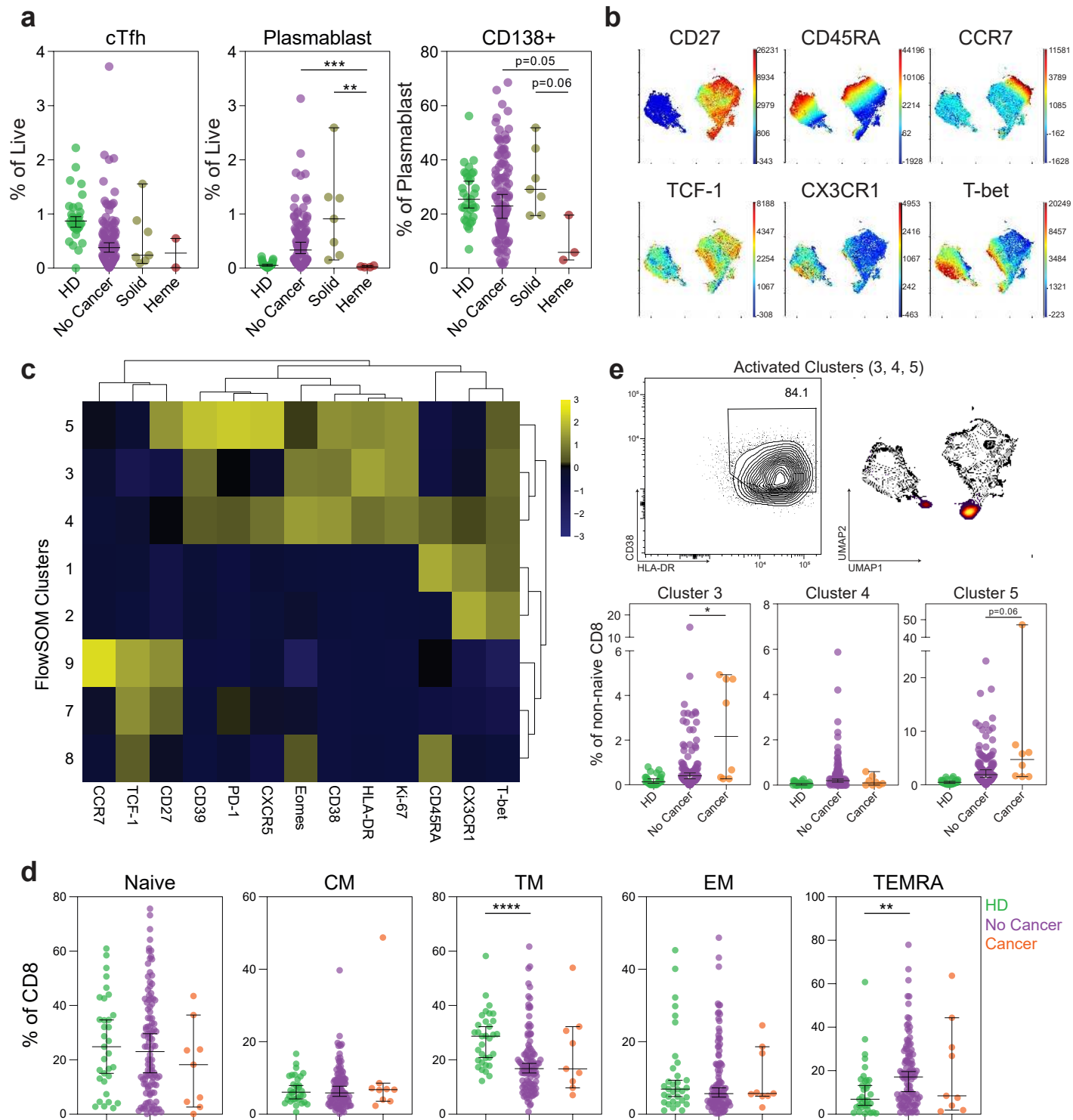
Extended Data Fig. 2 | SARS-CoV-2 antibody levels. (a) Relative levels of SARS-CoV-2 IgG and IgM in non-cancer (n=108) and cancer (n=21) patients. (b) Relative IgG levels in cancer patients. Each dot represents a cancer patient (Heme: Red; Solid: Yellow). (All) Significance determined by Mann Whitney test: *p<0.05, **p<0.01, ***p<0.001, and ****p<0.0001. Median and 95% CI shown.

Extended Data Fig. 3



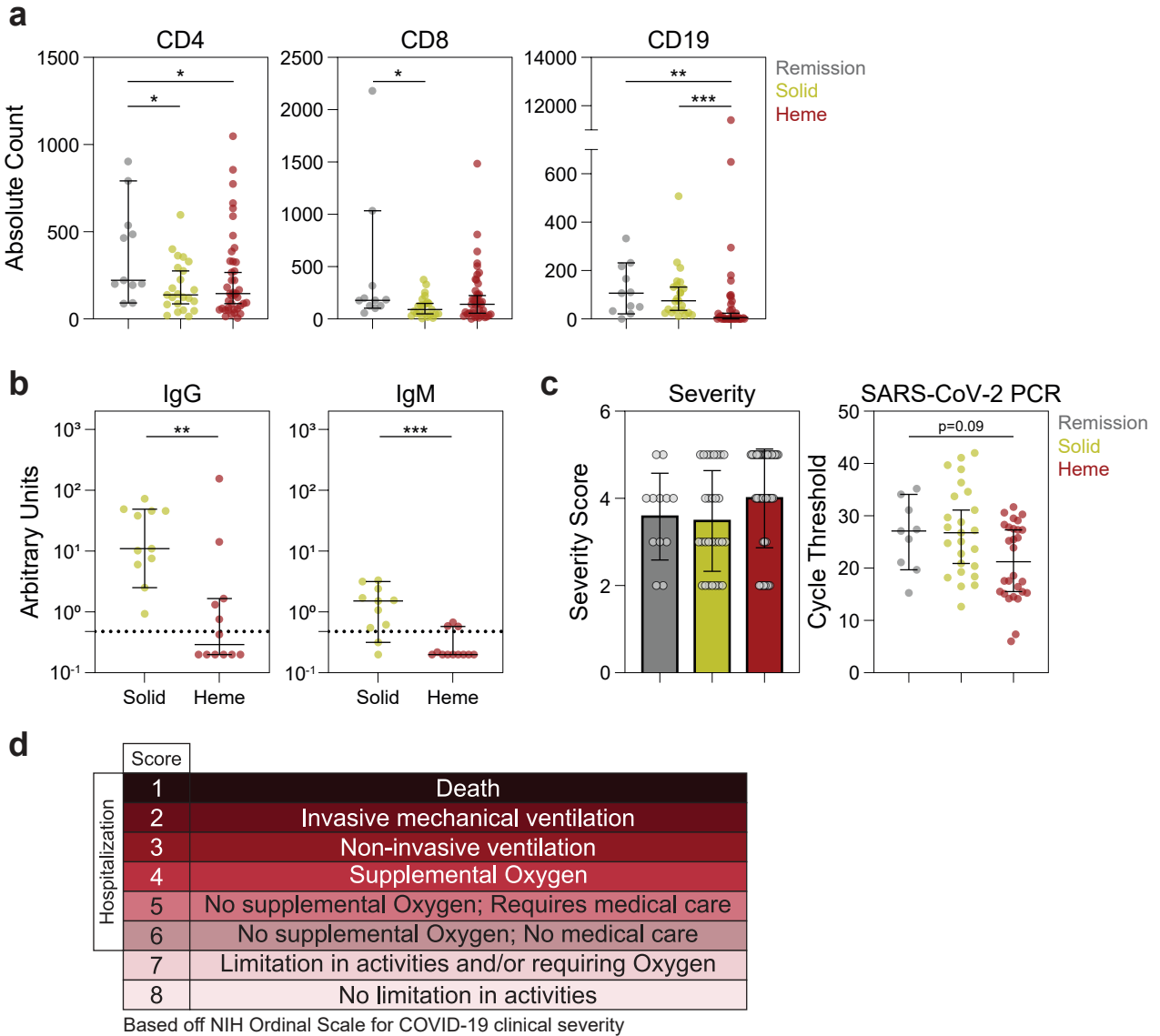
Extended Data Fig. 3 | Dimensionality reduction and EMD clustering of MESSI cohort. (a) UMAP projections of lymphocytes with indicated protein expression. **(b)** Frequencies of CD19+, CD3+, CD3+CD8+, and CD3+CD4+ cells of patients in each EMD cluster (Cluster 1 n=7; Cluster 2 n=16; Cluster 3 n=6; Cluster 4 n=10; Cluster 5 n=5). (All) Median and 95% CI shown.

Extended Data Fig. 4



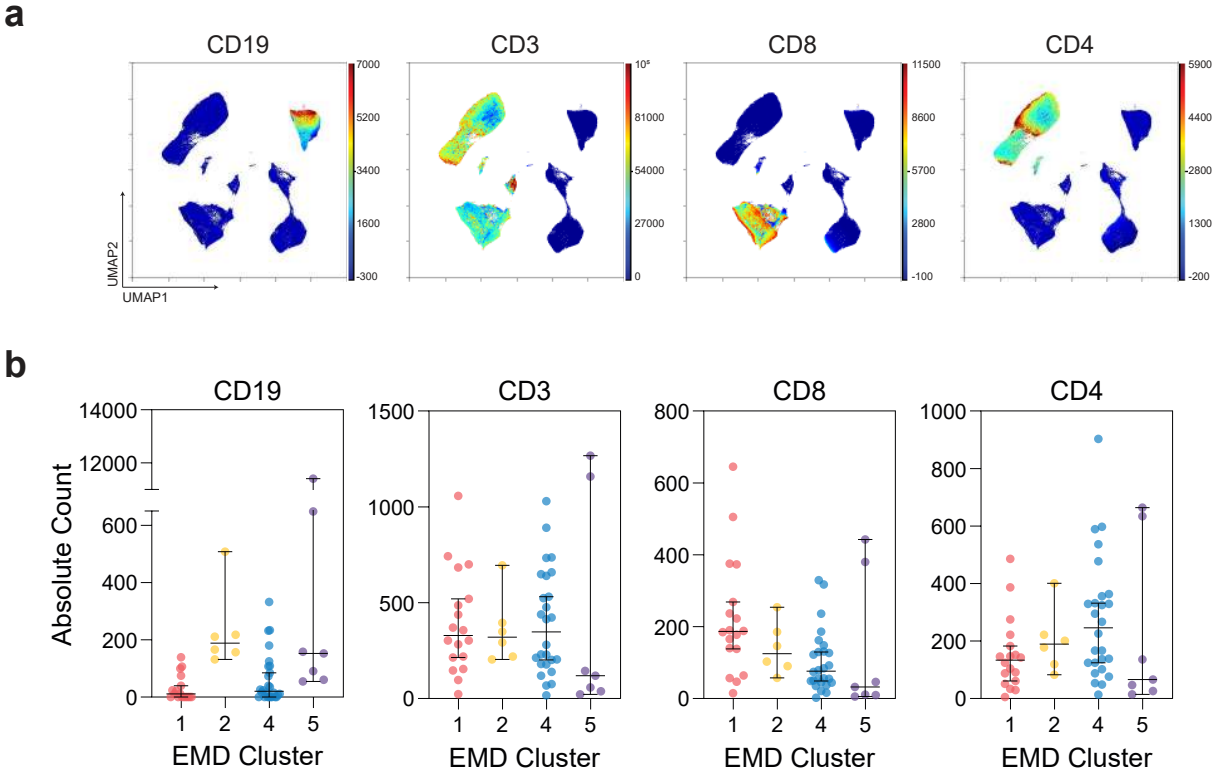
Extended Data Fig. 4 | Cellular phenotyping of COVID-19 patients with cancer. (a) Frequencies of circulating T follicular helper cells (cTfh), plasmablasts, and CD138 expression on plasmablasts (HD n=33; non-cancer n=108; solid cancer n=7; heme cancer n=3). (b) UMAP projection of non-naïve CD8 T cells with indicated protein expression. (c) Heatmap showing expression patterns of various markers, stratified by FlowSOM clusters. Heat scale calculated as column z-score of MFI. (d) Frequencies of CD8 subsets: naive (CD45RA+CD27+CCR7+), central memory (CD45RA-CD27+CCR7+), transition memory (CD45RA-CD27+CCR7-), effector memory (CD45RA-CD27-CCR7-), and TEMRA (CD45RA+CD27-CCR7-) (HD n=33; non-cancer n=108; cancer n=9). (e) (Top) HLA-DR and CD38 coexpression in concatenated activated clusters (3, 4, and 5) and associated UMAP localization. (Bottom) Frequency of activated clusters (3, 4, and 5) in each patient (HD n=30; non-cancer n=110; solid-cancer n=8). (All) Significance determined by Mann Whitney test: *p<0.05, **p<0.01, ***p<0.001, and ****p<0.0001. Median and 95% CI shown.

Extended Data Fig. 5



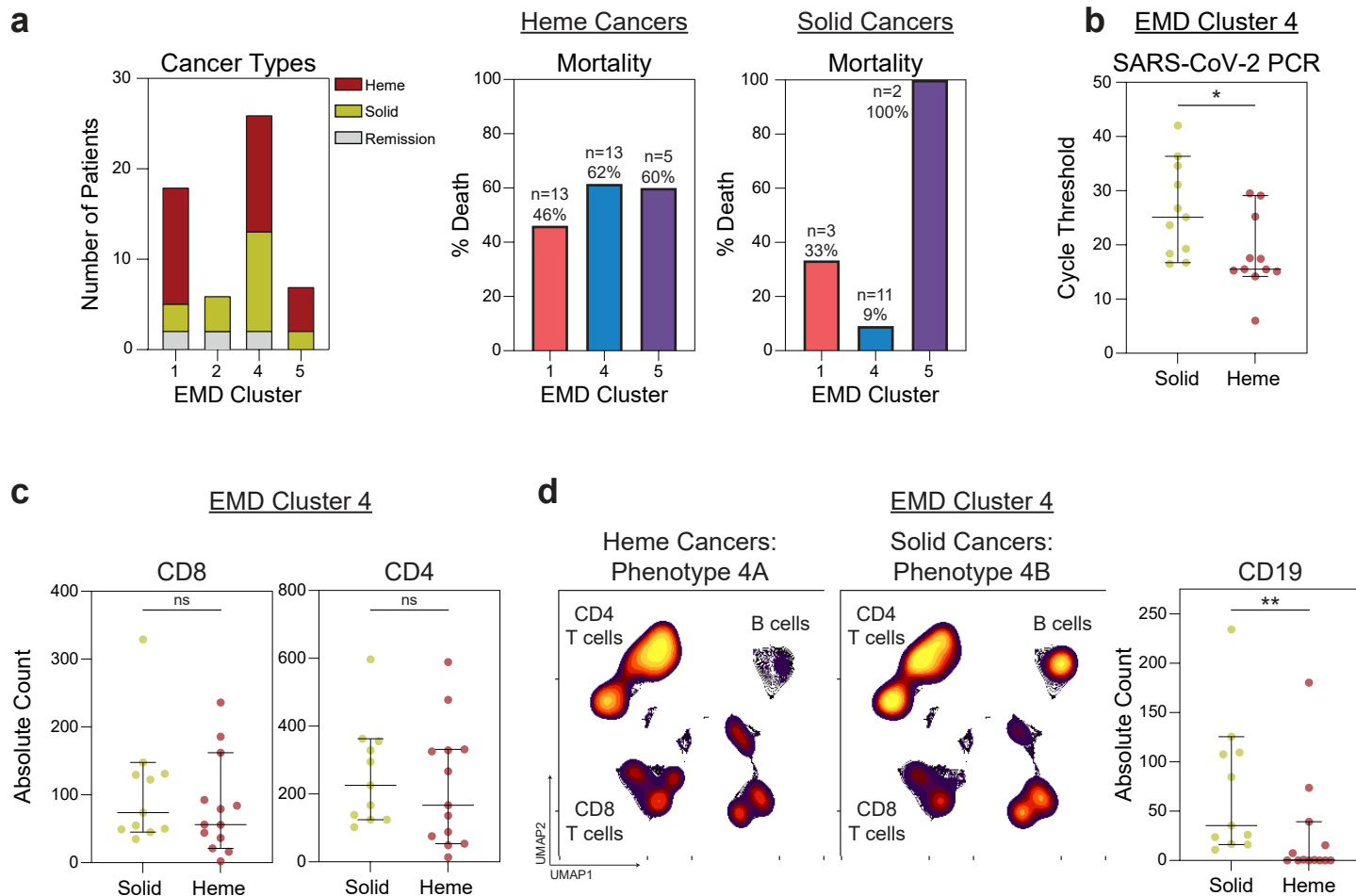
Extended Data Fig. 5 | Cellular, serologic, and clinical features in solid and hematologic cancer patients with COVID-19. (a) Absolute counts of CD4, CD8, and CD19 expression in remission (n=11), solid cancer (n=23), and hematologic cancer (n=41) patients. (b) Relative levels of SARS-CoV-2 IgG and IgM in solid (n=11) and hematologic cancer (n=14) patients. (c) Severity (NIH ordinal scale for COVID-19 clinical severity) and RT-PCR cycle threshold (remission n=9; solid n=25; heme n=28) (Lower Ct: Higher viral load). (d) NIH ordinal scale for COVID-19 clinical severity. (All) Significance determined by Mann Whitney test: *p<0.05, **p<0.01, ***p<0.001, and ****p<0.0001. Median and 95% CI shown.

Extended Data Fig. 6



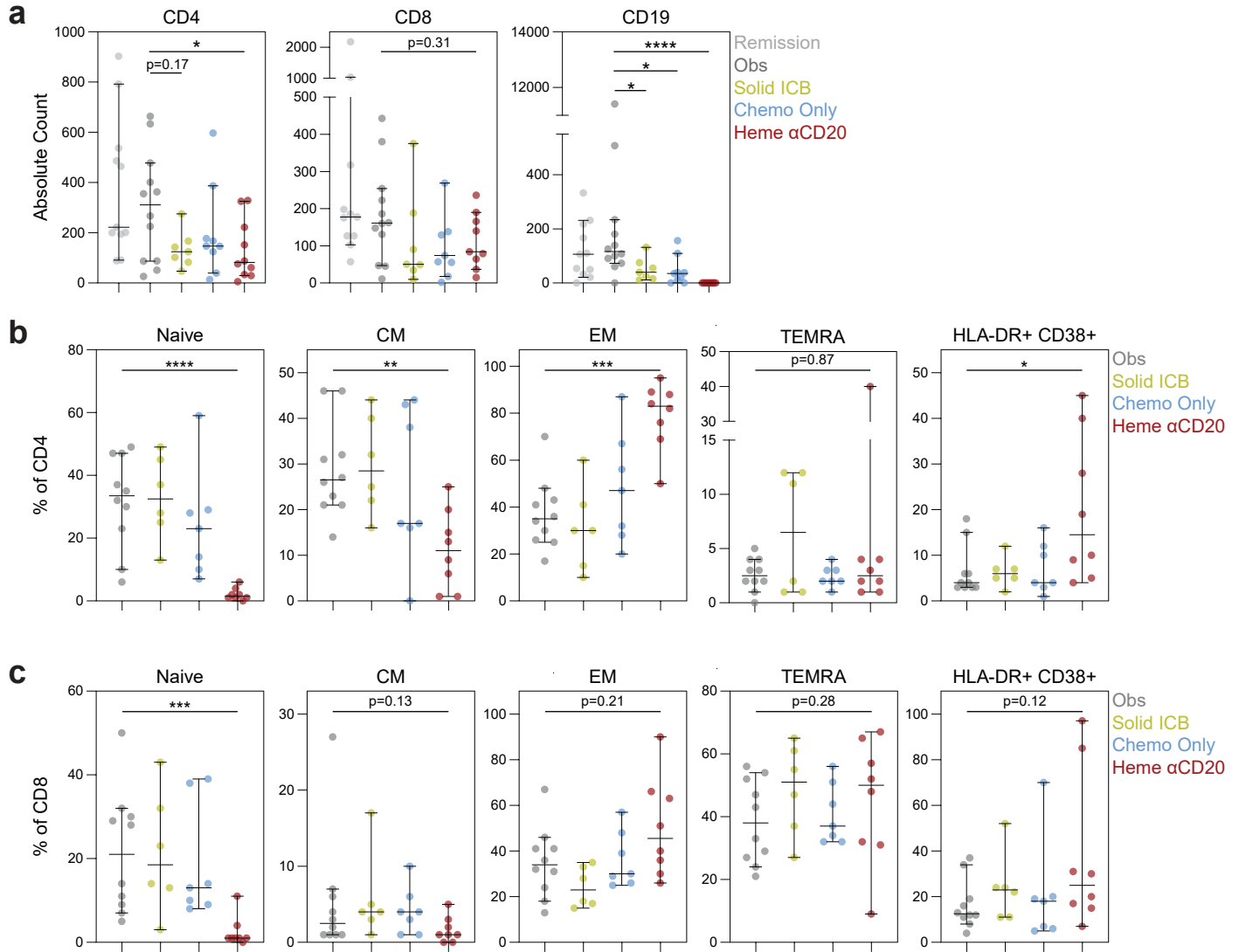
Extended Data Fig. 6 | Dimensionality reduction and EMD clustering of MSKCC cohort. (a) UMAP projections of lymphocytes with indicated protein expression. **(b)** Absolute counts of CD19+, CD3+, CD3+CD8+, and CD3+CD4+ cells of patients in each EMD cluster (Cluster 1 n=18; Cluster 2 n=6; Cluster 3 n=26; Cluster 4 n=7). (All) Median and 95% CI shown.

Extended Data Fig. 7



Extended Data Fig. 7 | EMD Cluster 4 drives differences in mortality between hematologic and solid cancer patients. (a) (Left) Number of patients with hematologic, solid, and remission cancer statuses within each EMD cluster. (Right) Mortality of patients within each EMD cluster for hematologic and solid cancers. (b) RT-PCR cycle threshold of solid and heme cancer patients in EMD cluster 4 (solid n=11; heme n=11). (c) Absolute CD8 and CD4 T cell counts for subjects in EMD cluster 4 stratified by solid (n=11) and heme (n=13) cancer. (d) Global UMAP projections of lymphocytes for subjects in EMD cluster 4: (Left) Hematologic cancer; (Middle) Solid cancer. (Right) Absolute B cell counts for subjects in EMD cluster 4 stratified by solid (n=11) and heme (n=13) cancer. (All) Significance determined by Mann Whitney test: *p<0.05, **p<0.01, ***p<0.001, and ****p<0.0001. Median and 95% CI shown.

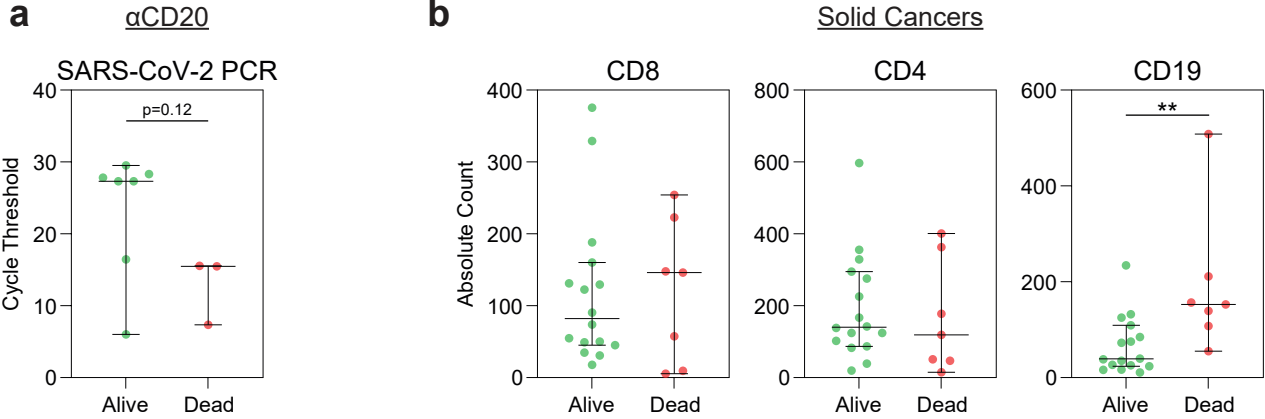
Extended Data Fig. 8



Extended Data Fig. 8 | Effect of cancer treatment on T cell differentiation in cancer patients with COVID-19. (a) Absolute counts of CD4, CD8, and CD19 expressing cells.

Frequencies of (b) CD4 and (c) CD8 T cell subsets in cancer patients treated with immune checkpoint blockade therapies, chemotherapies, and B cell depleting therapies. Naive (CD45RA+CCR7+), CM (CD45RA-CCR7+), EM (CD45RA-CCR7-), TEMRA (CD45RA+CCR7-). (All) Remission n=11, obs n=12, chemo only n=9, solid ICB n=7, and heme α CD20 n=10. Significance determined by Mann Whitney test: *p<0.05, **p<0.01, ***p<0.001, and ****p<0.0001. Median and 95% CI shown.

Extended Data Fig. 9



Extended Data Fig. 9 | Association of mortality with cell counts and viral load. (a) RT-PCR cycle threshold of patients treated with α CD20 therapy (alive n=7; dead n=3). **(b)** Absolute counts of CD8+, CD4+, and CD19+ cells in solid cancer patients (alive n=16; dead n=7). (All) Significance determined by Mann Whitney test: *p<0.05, **p<0.01, ***p<0.001, and ****p<0.0001. Median and 95% CI shown.

Supplementary Table 1 | COPE: Patient demographics and clinical characteristics by tumor type.

	Solid (N=78)	Heme (N=22)
Age, median (IQR)	70.5 (57-78)	64.5 (60-77)
Gender, female	39 (50.0%)	9 (40.9%)
Race		
White	24 (30.8%)	9 (40.9%)
Non-white	49 (62.8%)	12 (54.6%)
Unknown	5 (6.41%)	1 (4.55%)
Smoking History, Current/Prior	44 (56.4%)	13 (59.1%)
Comorbidities		
Cardiac	63 (80.8%)	15 (68.2%)
Pulmonary	38 (48.7%)	3 (13.6%)
Use of immunosuppressive drugs ⁺	23 (29.5%)	7 (31.8%)
BMI, median (IQR)	26.6 (23.2-30.9)	28.7 (24.0-33.4)
Cancer Status, Active ^{**}	32 (41.0%)	14 (63.6%)
Cancer Treatment		
Treatment in last 3 months		
Cytotoxic Chemotherapy	16 (20.5%)	8 (36.4%)
Hormone therapy	15 (19.2%)	0 (0.00%)
Active Surveillance/surgery	43 (55.1%)	10 (45.5%)
Other [*]	4 (5.13%)	4 (18.2%)
ECOG Performance Status	N=58	N=15
0-1	28 (48.3%)	9 (60.0%)
2	9 (15.5%)	4 (26.7%)
3-4	21 (36.2%)	2 (13.3%)
[*] Single agent immunotherapy, targeted therapy, monoclonal antibodies ⁺ Exposure to immunosuppressive medications not including cancer treatment ^{**} Diagnosis or treatment within 6 months		

Supplementary Table 2 | MESSI: Patient demographics and clinical characteristics by cancer status.

	Non-Cancer (N=108)	Cancer (N=22)	Overall (N=130)
Gender			
Female	49 (45.4%)	14 (63.6%)	63 (48.5%)
Male	59 (54.6%)	8 (36.4%)	67 (51.5%)
Age (median)	60	66	60.5
Race			
Asian	5 (4.6%)	1 (4.5%)	6 (4.6%)
Black	74 (68.5%)	16 (72.7%)	90 (69.2%)
White	28 (25.9%)	5 (22.7%)	33 (25.4%)
Pacific Islander	1 (0.9%)	0 (0%)	1 (0.8%)
Symptoms (Days before hospitalization) (median)	9	8	9
Severity (At hospitalization) (median)	3.5	3	3
Mortality (28 days)	12 (11.1%)	8 (36.4%)	20 (15.4%)

Supplementary Table 3 | MESSI: Patient demographics and clinical characteristics by cancer type.

	Heme (N=7)	Solid (N=15)	Overall (N=22)
Gender			
Female	4 (57.1%)	10 (66.7%)	14 (63.6%)
Male	3 (42.9%)	5 (33.3%)	8 (36.4%)
Age (median)	67	65	66
Race			
Asian	0 (0%)	1 (6.7%)	1 (4.5%)
Black	5 (71.4%)	11 (73.3%)	16 (72.7%)
White	2 (28.6%)	3 (20.0%)	5 (22.7%)
Symptoms (Days before hospitalization) (median)	9	7.5	8
Severity (At hospitalization) (median)	3	4	3
Mortality (28 days)	2 (28.6%)	6 (40.0%)	8 (36.4%)
COVID Treatments			
Remdesivir	1 (14.3%)	2 (13.3%)	3 (13.6%)
Convalescent Plasma	1 (14.3%)	3 (20.0%)	4 (18.2%)
Early Steroids	4 (57.1%)	5 (33.3%)	9 (40.9%)

Supplementary Table 4 | MESSI: Cancer type and cancer treatment.

	Heme (N=7)	Solid (N=15)	Overall (N=22)
Cancer Type			
CML	1 (14.3%)	0 (0%)	1 (4.5%)
CTCL	1 (14.3%)	0 (0%)	1 (4.5%)
Lymphoma	1 (14.3%)	0 (0%)	1 (4.5%)
Mantle Cell Lymphoma	1 (14.3%)	0 (0%)	1 (4.5%)
MM	1 (14.3%)	0 (0%)	1 (4.5%)
MPN	1 (14.3%)	0 (0%)	1 (4.5%)
Myeloma	1 (14.3%)	0 (0%)	1 (4.5%)
Bladder	0 (0%)	1 (6.7%)	1 (4.5%)
Breast	0 (0%)	6 (40.0%)	6 (27.3%)
GBM	0 (0%)	1 (6.7%)	1 (4.5%)
Head and Neck	0 (0%)	1 (6.7%)	1 (4.5%)
NSCLC	0 (0%)	1 (6.7%)	1 (4.5%)
Ovarian	0 (0%)	1 (6.7%)	1 (4.5%)
Pancreas	0 (0%)	1 (6.7%)	1 (4.5%)
Prostate	0 (0%)	2 (13.3%)	2 (9.1%)
SCLC	0 (0%)	1 (6.7%)	1 (4.5%)
Cancer Treatment			
αCD20 + Chemotherapy	1 (14.3%)	0 (0%)	1 (4.5%)
Chemo	5 (71.4%)	4 (26.7%)	9 (40.9%)
None	1 (14.3%)	1 (6.7%)	2 (9.1%)
Chemotherapy + Radiation	0 (0%)	1 (6.7%)	1 (4.5%)
Hormonal	0 (0%)	4 (26.7%)	4 (18.2%)
Hormonal + CDK Inhibitor	0 (0%)	1 (6.7%)	1 (4.5%)
Hormonal + Radiation	0 (0%)	1 (6.7%)	1 (4.5%)
ICB	0 (0%)	3 (20.0%)	3 (13.6%)

Supplementary Table 5 | MSKCC: Patient demographics and clinical characteristics by cancer type.

	Heme (N=45)	Solid (N=39)	Overall (N=84)
Gender			
Female	21 (46.7%)	20 (51.3%)	41 (48.8%)
Male	24 (53.3%)	19 (48.7%)	43 (51.2%)
Age (median)	64	66	65
Race			
Asian	2 (4.4%)	3 (7.7%)	5 (6.0%)
Black	5 (11.1%)	4 (10.3%)	9 (10.7%)
White	38 (84.4%)	30 (76.9%)	68 (81.0%)
Disease Severity (median)	4	3	4
Mortality (In hospital)	20 (44.4%)	8 (20.5%)	28 (33.3%)
COVID Treatments			
Remdesivir	12 (26.7%)	6 (15.4%)	18 (21.4%)
Convalescent Plasma	25 (55.6%)	14 (35.9%)	39 (46.4%)
Early Steroids	17 (37.8%)	21 (53.8%)	38 (45.2%)

Supplementary Table 6 | MSKCC: Cancer type and cancer treatment.

	Heme (N=45)	Solid (N=39)	Overall (N=84)
Cancer Type			
ALL	4 (8.9%)	0 (0%)	4 (4.8%)
AML	6 (13.3%)	0 (0%)	6 (7.1%)
CLL	4 (8.9%)	0 (0%)	4 (4.8%)
Lymphoma	23 (51.1%)	0 (0%)	23 (27.4%)
MDS/Myelofibrosis	3 (6.7%)	0 (0%)	3 (3.6%)
Myeloma	5 (11.1%)	0 (0%)	5 (6.0%)
Bladder	0 (0%)	2 (5.1%)	2 (2.4%)
Breast	0 (0%)	8 (20.5%)	8 (9.5%)
CNS	0 (0%)	3 (7.7%)	3 (3.6%)
Colorectal	0 (0%)	5 (12.8%)	5 (6.0%)
GYN	0 (0%)	3 (7.7%)	3 (3.6%)
Head and Neck	0 (0%)	1 (2.6%)	1 (1.2%)
Kidney	0 (0%)	1 (2.6%)	1 (1.2%)
Liver	0 (0%)	1 (2.6%)	1 (1.2%)
Lung	0 (0%)	5 (12.8%)	5 (6.0%)
Melanoma	0 (0%)	2 (5.1%)	2 (2.4%)
Prostate	0 (0%)	3 (7.7%)	3 (3.6%)
Renal	0 (0%)	1 (2.6%)	1 (1.2%)
Sarcoma	0 (0%)	2 (5.1%)	2 (2.4%)
Thymoma	0 (0%)	1 (2.6%)	1 (1.2%)
Thyroid	0 (0%)	1 (2.6%)	1 (1.2%)
Cancer Treatment			
αCD20	9 (20.0%)	0 (0%)	9 (10.7%)
αCD20 + chemo	9 (20.0%)	0 (0%)	9 (10.7%)
anti-CD30	1 (2.2%)	0 (0%)	1 (1.2%)
αHER2	0 (0%)	2 (5.1%)	2 (2.4%)
AXL inhibitor	1 (2.2%)	0 (0%)	1 (1.2%)
Bispecific	1 (2.2%)	0 (0%)	1 (1.2%)
BTK inhibitor	4 (8.9%)	0 (0%)	4 (4.8%)
CAR-T	1 (2.2%)	0 (0%)	1 (1.2%)
Chemotherapy	8 (17.8%)	15 (38.5%)	23 (27.4%)
EZH inhibitor	1 (2.2%)	0 (0%)	1 (1.2%)
PI3K Inhibitor	1 (2.2%)	0 (0%)	1 (1.2%)
Proteasome inhibitor	3 (6.7%)	0 (0%)	3 (3.6%)
Radiation	1 (2.2%)	0 (0%)	1 (1.2%)
Tyrosine kinase inhibitor	1 (2.2%)	0 (0%)	1 (1.2%)
Hormonal	0 (0%)	5 (12.8%)	5 (6.0%)
Immune checkpoint blockade	0 (0%)	7 (17.9%)	7 (8.3%)
VEGF inhibitor	0 (0%)	1 (2.6%)	1 (1.2%)
None	4 (8.9%)	9 (23.1%)	13 (15.5%)

Figures

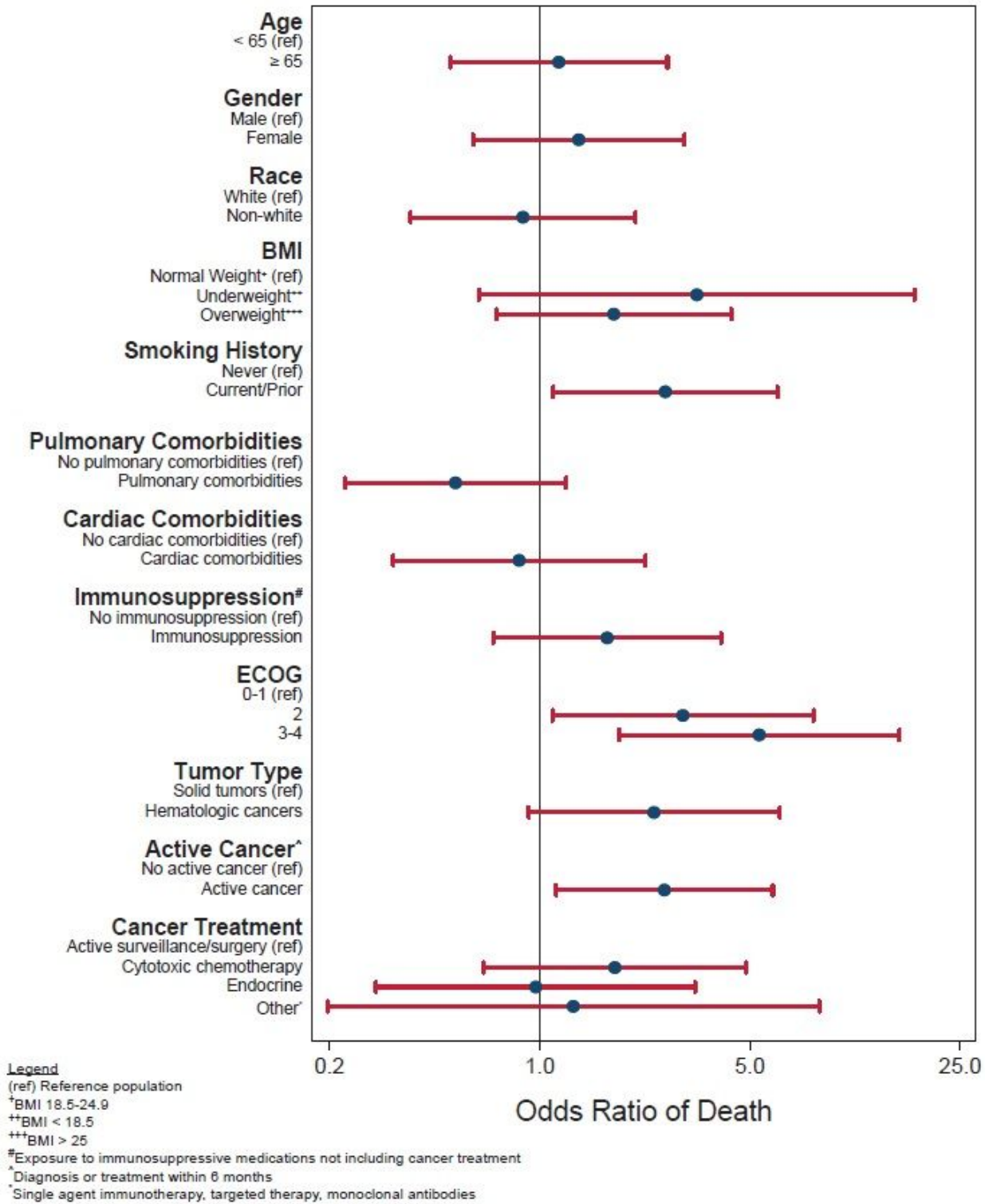


Figure 1

Univariate analysis of potential risk factors in COVID-19 mortality.

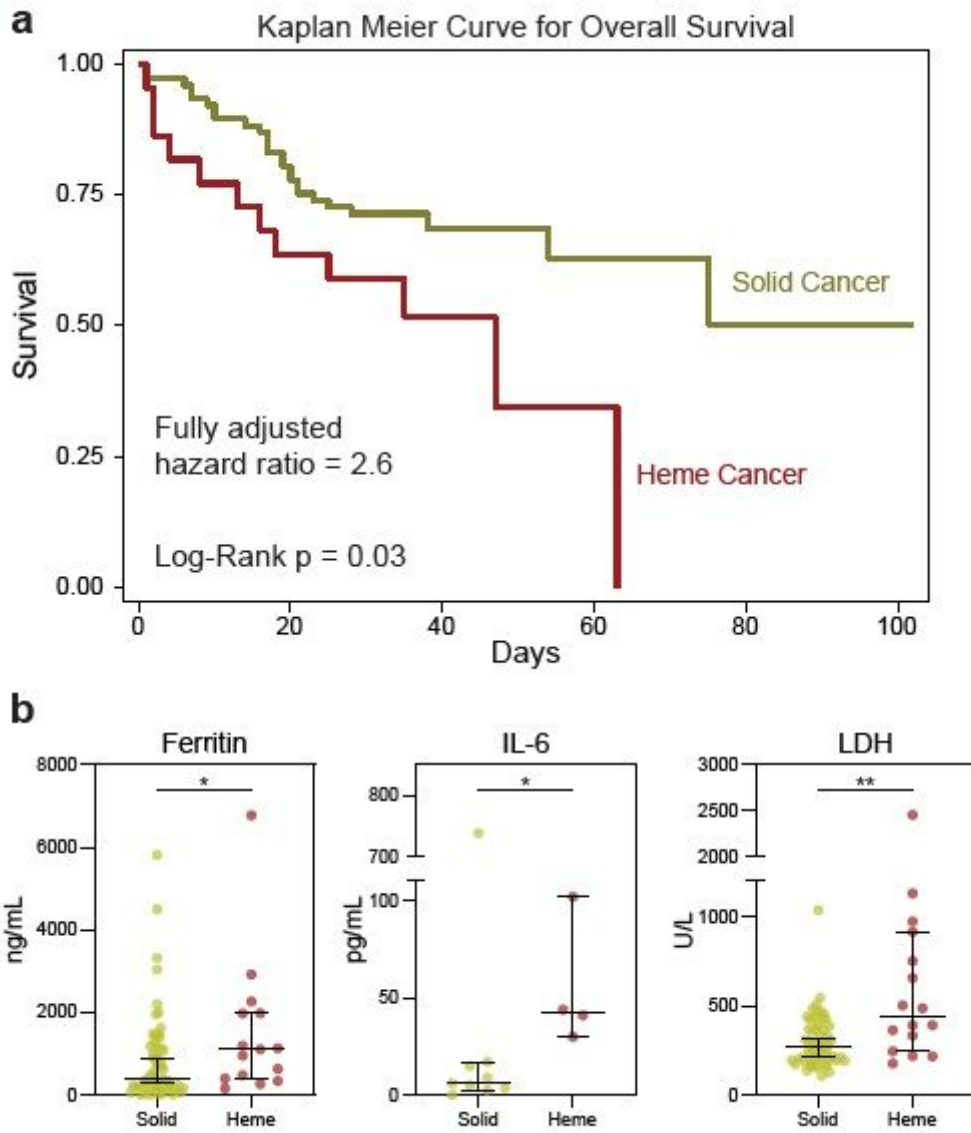


Figure 2

Hematologic cancer is an independent risk factor for COVID-19 related mortality. (a) Kaplan Meier curve for COVID-19 survival of patients with solid (n=77) and hematologic (n=22) cancer. Cox regression-computed hazard ratio for mortality in hematologic vs solid cancer, adjusted for age, gender, smoking status, active cancer status, and ECOG performance status. (b) Ferritin, IL-6, and LDH in solid (n=62) and hematologic (n=15) cancer hospitalized for COVID-19. (All) Significance determined by Mann Whitney test: * $p < 0.05$, ** $p < 0.01$, *** $p < 0.001$, and **** $p < 0.0001$. Median and 95% CI shown.

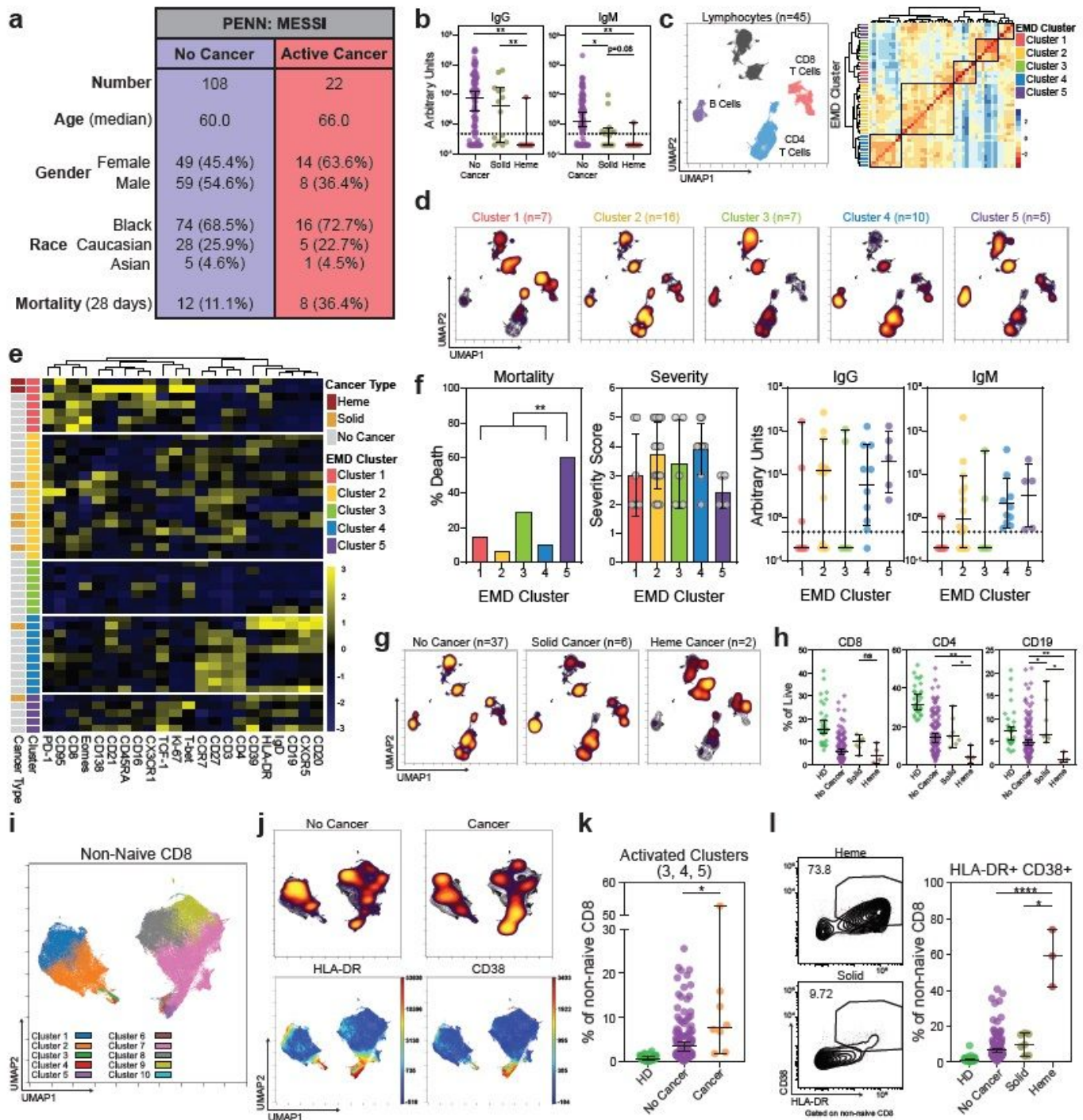


Figure 3

High dimensional analyses reveal immune phenotypes associated with mortality and distinct phenotypes between solid and hematologic cancers. (a) Demographic and mortality data for MESSI cohort at Penn. (b) Relative levels of SARS-CoV-2 IgG and IgM of solid (n=14) and hematologic (n=7) cancer patients and non-cancer patients (n=108). (c) (Left) Global UMAP projection of lymphocyte populations for all 45 patients pooled. (Right) Hierarchical clustering of Earth Mover's Distance (EMD) using Pearson correlation, calculated pairwise for lymphocyte populations. (d) UMAP projection of concatenated lymphocyte populations for each EMD cluster. (Yellow: High Density; Black; Low Density)

(e) Heatmap showing expression patterns of various markers, stratified by EMD cluster. Heat scale calculated as column z-score of MFI. (f) Mortality, disease severity, and SARS-CoV-2 antibody data, stratified by EMD cluster (Cluster 5 n=5; Cluster 1,2,3,4 n=40). Mortality significance determined by Pearson Chi Square test. Severity assessed with NIH ordinal scale for COVID-19 clinical severity (1: Death; 8: Normal Activity)¹⁵. (g) UMAP projections of concatenated lymphocyte populations for solid cancer, hematologic cancer, and non-cancer patients. (h) CD8 and CD4 T cell and B cell frequencies in healthy donors (HD) (n=33), non-cancer (n=108), solid cancer (n=7), and heme cancer (n=4). (i) UMAP projection of non-naïve CD8 T cell clusters identified by FlowSOM. (j) (Top) UMAP projections of non-naïve CD8 T cells for non-cancer and cancer patients. (Bottom) UMAP projections indicating HLA-DR and CD38 protein expression on non-naïve CD8 T cells for all patients pooled. (k) Frequency of activated FlowSOM clusters in HD (n=30), non-cancer (n=110), and cancer patients (n=8). (l) Representative flow plots and frequency of HLA-DR and CD38 co-expression in HD (n=30), non-cancer (n=110), solid cancer (n=7), and hematologic cancer (n=3) patients. (All) Significance determined by Mann Whitney test: *p<0.05, **p<0.01, ***p<0.001, and ****p<0.0001. Median and 95% CI shown.

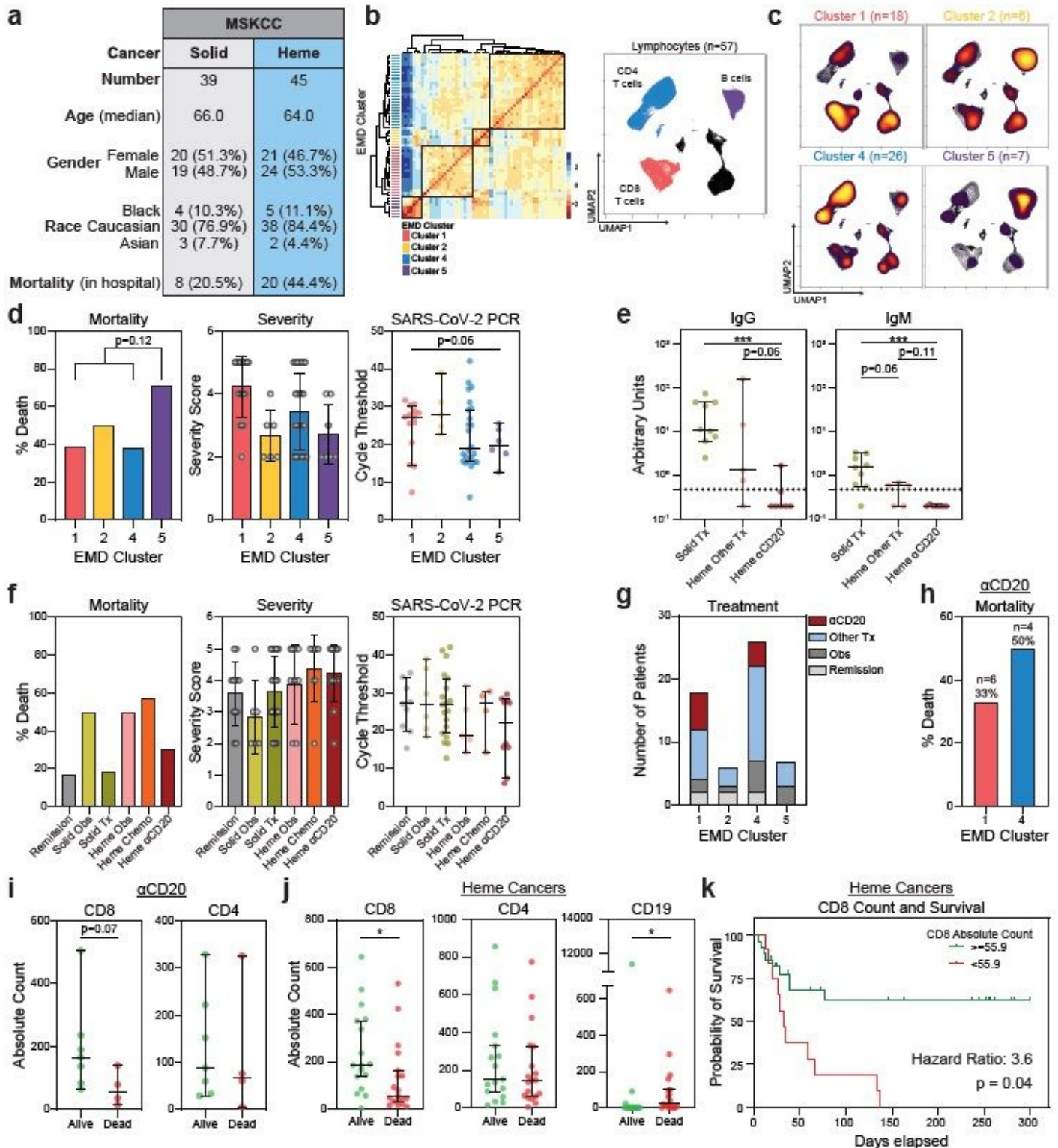


Figure 4

CD8 T cell counts associated with survival in hematologic cancer patients with COVID-19. (a) Demographic and mortality data of MSKCC cohort. (b) (Left) Hierarchical clustering of Earth Mover's Distance (EMD) using Pearson correlation, calculated pairwise for lymphocyte populations. (Right) Global UMAP projection of lymphocyte populations pooled. (c) UMAP projection of concatenated lymphocyte populations for each EMD cluster. (Yellow: High Density; Black: Low Density) (d) Mortality

(Cluster 5 n=7; Cluster 1,2,4 n=50), severity, and RT-PCR cycle threshold (Cluster 1 n=14; Cluster 2 n=5; Cluster 4 n=24; Cluster 5 n=6) (Lower Ct: Higher viral load) stratified by EMD cluster. Mortality significance determined by Pearson Chi Square test. (e) Relative levels of SARS-CoV-2 IgG and IgM of patients with recent cancer treatments (solid tx n=9; heme α CD20 n=7; heme other tx n=5). (f) Mortality, severity, and RT-PCR cycle threshold stratified by cancer treatment (remission n=9; solid obs n=6; solid tx n=19; heme obs n=5; heme chemo n=4; heme α CD20 n=10). Severity assessed with NIH ordinal scale for COVID-19 clinical severity. (g) Recent cancer treatment of patients in each EMD cluster. (h) Mortality of patients treated with B cell depleting therapy in EMD cluster 1 (red) and EMD cluster 4 (blue). (i) Absolute CD8 and CD4 T cell counts in patients treated with B cell depleting therapy (alive n=7; dead n=4). (j) Absolute CD8 and CD4 T cell counts and B cell counts in hematologic cancer patients (alive n=17; dead n=18). (k) Kaplan-Meier curve for survival in hematologic cancer patients stratified by CD8 T cell counts (threshold = 55.9; log-rank hazard ratio) (≥ 55.9 n=28; < 55.9 n=13). CD8 count threshold determined by Classification and Regression Tree (CART) analysis. (All) Significance determined by Mann Whitney test: *p<0.05, **p<0.01, ***p<0.001, and ****p<0.0001. Median and 95% CI shown.